

2021

TECH LIBRARY
KAFB, NM



NATIONAL ADVISORY COMMITTEE FOR AERONAUTICS

8152

TECHNICAL NOTE

NO. 1702

ANALYTICAL AND EXPERIMENTAL PERFORMANCE OF AN EXPLOSION-CYCLE COMBUSTION CHAMBER FOR A JET-PROPULSION ENGINE

By Morris A. Zipkin and George W. Lewis, Jr.

Flight Propulsion Research Laboratory
Cleveland, Ohio



Washington
September 1948

AFMBC
TECHNICAL LIBRARY
AFL 2811



0144963

NATIONAL ADVISORY COMMITTEE FOR AERONAUTICS

TECHNICAL NOTE NO. 1702

ANALYTICAL AND EXPERIMENTAL PERFORMANCE OF AN
EXPLOSION-CYCLE COMBUSTION CHAMBER FOR
A JET-PROPULSION ENGINE

By Morris A. Zipkin and George W. Lewis, Jr.

SUMMARY

The results of analytical and experimental investigations of the performance of an explosion-cycle combustion chamber are presented. Calculated and experimentally determined explosion-pressure ratios obtained in a combustion chamber with a timed inlet valve and several fixed-area exhaust nozzles are presented over a range of fuel-air ratios. The effects on explosion-pressure ratio of variations in cycle frequency and inlet pressure are investigated. Calculated and experimental values of jet thrust and thrust specific fuel consumption obtained from this combustion chamber are also included.

It was found that for the configuration investigated, the combustion time varied from 0.003 to 0.009 second with values in the region of 0.006 being most predominant. Calculated explosion-pressure ratios and jet thrust based on a combustion time of 0.006 second indicated that explosion-pressure ratio would range from 1.7 to 5.0 and jet thrust from 15 to 40 pounds per pound of air per second, depending on the fuel-air ratio and the ratio of exhaust-nozzle area to combustion-chamber cross-sectional area with maximum values occurring at approximately stoichiometric fuel-air ratio. Maximum experimental values of explosion-pressure ratio and jet thrust, approximately 2.9 and 35 pounds per pound of air per second, respectively, occurred at an over-all fuel-air ratio of about 0.04. Lower values of explosion-pressure ratio and thrust per pound of air were obtained for fuel-air ratios richer or leaner than approximately 0.04. The calculations indicated that if combustion time could be reduced from 0.006 to 0.003 second, explosion pressure ratios could be increased by more than 30 percent and thrust per pound of air per second increased by approximately 100 percent.

INTRODUCTION

The use of engines operating on the constant-volume cycle offers, at least theoretically, a means of improving the performance of jet-propulsion units. The constant-volume cycle possesses certain theoretical advantages over the more commonly used constant-pressure cycle, namely, higher ideal efficiency and output per pound of air handled per unit time. Actual performance of a constant-volume jet engine, however, would depend upon the extent to which constant-volume combustion could be approached and the resulting explosion pressure developed in the combustion chamber. An investigation of the performance of an explosion-cycle combustion chamber would therefore serve as an indication of the performance that can be expected from a jet engine utilizing this cycle.

In the Holzwarth turbine described in reference 1, the principles of the constant-volume cycle are applied to a large stationary gas turbine. This engine develops pressure ratios higher than 5 in its explosion-type combustion chamber. These high pressure ratios are obtained by the use of valves in both the inlet and exhaust ports of the combustion chamber. In order to avoid the complications involved in the use of exhaust valves, the constant-volume cycle can be approximated by use of only an inlet valve and a fixed exit nozzle; the smaller the nozzle area the more nearly the ideal cycle is approached.

The results of analytical and experimental investigations conducted at the NACA Cleveland laboratory to determine the performance of an explosion-cycle combustion chamber with a timed inlet valve and several fixed-area exhaust nozzles are presented herein. Experimentally determined explosion-pressure ratios, thrust per pound of air, and specific fuel consumption are presented as functions of fuel-air ratio, ratio of exhaust-nozzle area to combustion-chamber cross-sectional area, cycle frequency, and inlet pressure. These values are compared with theoretical values obtained from an analysis of an ideal constant-volume cycle and an approximate constant-volume cycle, which is also presented.

This analysis is not applicable to a pulse-jet engine of the type used in the German V-1 bomb. Preliminary analyses of that engine have been made based on the constant-volume cycle but it has been shown (reference 2) that such analyses are not in good agreement with the actual physical phenomena that occur.

ANALYSIS

This section is limited to a discussion of the significance of the derived equations, inasmuch as a complete cycle analysis is presented in appendix B. (The symbols used are defined in appendix A.)

An analysis of the general energy equation for the combustion process in an explosion chamber having a fixed-area exhaust nozzle was made in order to estimate the explosion temperature and pressure developed. On the basis of the assumptions given in appendix A, it can be shown that the maximum temperature ratio developed during the combustion process can be obtained from a graphical integration of the following equation:

$$\int_1^{T_3/T_2} \frac{d\left(\frac{T}{T_2}\right)}{\frac{J}{RT_0} \left(\gamma-1\right) \left(\frac{T_0}{T_2}\right) \left(\frac{f/a}{f/a+1}\right) \left(\frac{h}{t_0}\right) - \left(\gamma-1\right) \left(\frac{A_e}{A_b}\right) \left(\frac{l}{L}\right) \left(\frac{2\gamma g RT_0}{\gamma+1}\right)^{1/2} \left(\frac{T}{T_2}\right)^{3/2} \left(\frac{T_2}{T_0}\right)^{1/2} \left(\frac{2}{\gamma+1}\right)^{\frac{1}{\gamma-1}}} = \int_0^{t_c} dt$$

Similarly it is possible to show that the maximum pressure ratio and the maximum temperature ratio developed during the combustion process can be related by the following equation:

$$\log_e \left(\frac{P_3}{P_2}\right) = \log_e \left(\frac{T_3}{T_2}\right) - \int_1^{T_3/T_2} \frac{\frac{1}{\gamma-1} \left(\frac{T}{T_2}\right)^{1/2} d\left(\frac{T}{T_2}\right)}{\left(\frac{A_b}{A_e}\right) L \left(\frac{f/a}{f/a+1}\right) \left(\frac{h}{t_0}\right) \left(\frac{J}{RT_0}\right) \left(\frac{T_0}{T_2}\right)^{3/2} \left(\frac{\gamma+1}{2}\right)^{\frac{1}{2(\gamma-1)}} \left(\frac{1}{\gamma g RT_0}\right)^{1/2} - \left(\frac{T}{T_2}\right)^{3/2}}$$

The thrust output per pound of air flow per unit time obtained from a consideration of the impulse during the cycle is equal to:

$$\frac{F}{W_a} = \frac{\sqrt{\gamma g R T_0}}{\gamma g} \left(\frac{2}{\gamma - 1} \right)^{1/2} \left(\frac{T_2}{T_0} \right)^{1/2} \left(\frac{T_2}{T_3} \right)^{1/2} \left(\frac{P_3}{P_2} \right) \left\{ \int_{P_0/P_3}^1 \left(\frac{P}{P_3} \right)^{\frac{1-\gamma}{\gamma}} \left[\left(\frac{P}{P_3} \right)^{\frac{\gamma-1}{\gamma}} - \left(\frac{P_0}{P_3} \right)^{\frac{\gamma-1}{\gamma}} \right]^{1/2} d\left(\frac{P}{P_3} \right) \right. \\ \left. + \gamma \left(\frac{P_0}{P_3} \right)^{\frac{\gamma+1}{2}} \left[\left(\frac{P_2}{P_0} \right)^{\frac{\gamma-1}{\gamma}} - 1 \right]^{1/2} \right\}$$

and the thrust specific fuel consumption can be shown to equal

$$tsfc = \frac{3600 f/a}{F/W_a}$$

In order to determine the comparative time for combustion, blowdown, and purging of the combustion chamber and to estimate the range of cycle frequencies to be investigated, it was necessary to evaluate the time for one cycle. This time was taken as the sum of the time intervals required for combustion, blowdown, and purging of the combustion chamber. Charging of the chamber was assumed to occur simultaneously with purging. The time for one cycle can be shown to equal

$$t_n = \left(\frac{A_b}{A_e} \right) \frac{L}{\sqrt{\gamma g R T_0}} \left(\frac{T_0}{T_3} \right)^{1/2} \left(\frac{P_3}{P_0} \right)^{\frac{\gamma-1}{2\gamma}} \left(\frac{\gamma-1}{2} \right)^{1/2} \left\{ \left(\frac{\gamma+1}{2} \right)^{\frac{1}{\gamma-1}} \left(\frac{2}{\gamma-1} \right)^{3/2} \left[1 - \left(\frac{P_0}{P_3} \right)^{\frac{\gamma-1}{2\gamma}} \left(\frac{\gamma+1}{2} \right)^{1/2} \right] + \frac{1}{\gamma} \right. \\ \left. \int_1^{\left(\frac{\gamma+1}{2} \right)^{\frac{\gamma}{\gamma-1}}} \frac{\frac{d}{dp} \left(\frac{p}{P_0} \right)}{\left(\frac{p}{P_0} \right)^{\frac{\gamma-1}{\gamma}} \left[\left(\frac{p}{P_0} \right)^{\frac{\gamma-1}{\gamma}} - 1 \right]^{1/2}} + \left[\left(\frac{P_2}{P_0} \right)^{\frac{\gamma-1}{\gamma}} - 1 \right]^{-1/2} \right\} + t_o$$

and the calculated cycle frequency then equals

$$n = \frac{1}{t_n}$$

In actual operation, cycle frequency was varied over a wide range by varying the rotative speed of the inlet valve.

An examination of these equations shows that the performance of a combustion chamber of a jet-propulsion engine operating on the explosion cycle is a function of fuel-air ratio, ratio of exhaust-nozzle area to combustion-chamber cross-sectional area, combustion-chamber length, combustion time, and inlet pressure.

Analytical and experimental data are presented to show how explosion pressure ratio, thrust per pound of air, and specific fuel consumption vary with changes in fuel-air ratio, ratio of nozzle area to combustion-chamber cross-sectional area, cycle frequency, and inlet pressure. The analysis of combustion-chamber performance was made using an average time of combustion estimated from pressure-time curves obtained from the engine being investigated. Calculations were also made for two other combustion times in order to determine the effects of combustion time on the performance of the unit.

963

APPARATUS

Engine setup. - The investigation was conducted on an explosion-cycle combustion chamber, shown in figures 1 and 2. The test equipment consisted of a stationary 16-inch hub that housed a rotating ring valve and supported a stationary combustion chamber 2 feet in length. Radial clearance between the hub and the valve was approximately 0.012 inch. The ring valve acted as the inlet valve to the combustion chamber and the effective inlet-valve area could be varied by changing the size of the openings in the ring valve. For the investigation, the ports in the ring valve were so dimensioned that the inlet valve was either partly or fully opened for approximately 45 percent of the cycle. This value was chosen after theoretical analysis had shown that for the configuration being investigated the charging or purging period should be approximately 50 percent of the total cycle time. The ring valve was driven by a direct-current motor; one revolution of the valve corresponded to two cycles of the engine. Exhaust gases from the combustion chamber were discharged through a removable exit nozzle that made it possible to change the exhaust area by changing exit nozzles.

It was realized that the combustion chamber used for the investigation would have high entrance and exit losses because of the right-angle turns at the inlet and exhaust sections. (See fig. 2.) This configuration was used, however, because it was readily available.

Fuel and ignition systems. - Fuel was intermittently (once per cycle) injected into the combustion chamber by means of an injection pump through spring-loaded fuel nozzles. The fuel pump was chain-driven from the motor shaft. Fuel-injection timing was varied with respect to inlet-valve closing by the use of a phase changer included in the fuel-pump drive. Fuel flow was measured by means of a calibrated rotameter upstream of the injection pump. The fuel was injected into the combustion chamber in a direction counter to the air flow.

Two types of ignition system were used. Continuous ignition was obtained by direct connection of the spark plug to a 6000-volt transformer. Intermittent ignition was obtained by placing a circuit breaker and a capacitor in series with the power supply to the transformer. Spark plugs were located in several places on the combustion chamber in order to determine experimentally the best spark-plug location.

Thrust measurements. - Exhaust-gas thrust measurements were made by means of a thrust target and an NACA balanced-diaphragm torque cell, shown schematically in figure 2. A complete description of the type of thrust target used is given in reference 3.

Induction and exhaust systems. - Combustion air was supplied to the engine from the central laboratory system. Air flow was measured by means of a thin-plate orifice installed in the combustion air system according to A.S.M.E. standards.

The exhaust gases discharged into the thrust target and then were cooled by a water spray before entering the laboratory atmospheric-exhaust system.

Instrumentation. - Maximum and minimum cycle pressures were measured with an NACA balanced-diaphragm pressure indicator. Pressure-time diagrams were obtained from a link-coupled capacitor-type pressure indicator and a cathode-ray oscilloscope. Combustion-chamber inlet and exhaust pressures were measured by means of static-pressure taps installed in the inlet surge tank and in the thrust target, respectively. Combustion-air temperature was measured by an unshielded thermocouple located in the inlet surge tank.

PROCEDURE

The effects on engine performance of changes in fuel-air ratio, ratio of exhaust-nozzle area to combustion-chamber cross-sectional area, inlet-pressure ratio, and cycle frequency were determined by a series of engine investigations. For each investigation, inlet pressure ratio, cycle frequency, and nozzle area were fixed at constant values and the fuel flow was varied over a wide range. Before any data were taken, optimum fuel-injection timing was determined by varying the phase-changer setting until the maximum pressure rise was obtained. At each experimental point, the measured thrust was recorded and maximum and minimum cycle pressures were determined. Representative photographs were taken of the pressure-time diagrams indicated on the oscilloscope screen. The following ranges of conditions were investigated.

Fuel-air ratio	0.020 - 0.074
Cycle frequency, cycles/sec	^a ₁₅ - 40
Inlet pressure ratio	1.10 - 1.25
Ratio of exhaust-nozzle area to combustion-chamber cross-sectional area	1/9 - 1/3

^aA frequency of 15 cycles per second was the lowest that could be investigated with the apparatus used.

RESULTS AND DISCUSSION

Pressure-Time Diagrams

Variation in cycle pressure as a function of time is shown in figure 3. A pressure-time diagram of the theoretical cycle is shown in figure 3(a) and actual pressure-time curves obtained at various engine operating conditions are shown in figures 3(b) to 3(d). The sequence of operations can be readily followed on the ideal pressure-time curve. At the time the inlet valve opens, the pressure in the combustion chamber rises to inlet pressure (point 1). The chamber pressure then remains constant during the charging period, purging of the chamber occurring simultaneously with charging. At the end of the charging period (point 2), the inlet valve is closed, fuel is injected and combustion occurs with a resulting rapid increase in pressure (point 3). After combustion the cycle is completed with blowdown to approximately atmospheric pressure (point 4).

The actual pressure-time diagram deviated from the ideal in several respects, as can be seen in figures 3(b) to 3(d). At the time the inlet valve opens in the actual cycle, the pressure in the chamber rises to some intermediate value between ambient and inlet pressures. The actual value of the chamber pressure will be determined by the inlet pressure, the ratio of exhaust-nozzle area to combustion-chamber cross-sectional area, and the cycle frequency. Charging of the chamber occurs at essentially constant pressure but at the end of the charging period the pressure in the chamber falls off as the inlet valve closes. This loss in pressure results in a lower peak pressure at the end of the combustion process.

In the actual cycle, fuel is added to the chamber during the last part of the charging period rather than at the end of the charging period, as is assumed in the ideal cycle. It was found in the course of the investigation that the combustion-pressure rise was extremely sensitive to the timing of the fuel-injection period. For the experimental configuration used, the maximum

pressure rise was obtained when the fuel injection began approximately 20° before inlet closing. It was also found in the investigation that the pressure-time curves were unaltered by a change from intermittent to continuous ignition. After the engine had been operating for a short time, spark ignition was no longer necessary under most operating conditions.

The performance of any unit operating on the explosion cycle is dependent upon the pressure rise in the combustion chamber during the combustion or explosion process. The explosion-pressure rise is discussed on a nondimensional explosion-pressure-ratio basis; the explosion-pressure ratio is the ratio of maximum chamber pressure to the pressure in the chamber at the end of the charging period. For the theoretical case, explosion-pressure ratio would be equal to the ratio of maximum cycle pressure to inlet pressure. In the experimentally determined explosion-pressure ratios, the chamber pressure at the end of charging was a variable. For the larger nozzles investigated (ratios of exhaust-nozzle area to combustion-chamber cross-sectional area of $1/4$ and $1/3$), the chamber pressure was reduced to ambient pressure before combustion began. (See fig. 3(d).)

Factors Affecting Explosion-Pressure Ratio

It was shown in the analysis that the explosion-pressure ratio is a function of combustion time, fuel-air ratio, ratio of exhaust-nozzle area to combustion-chamber cross-sectional area, inlet pressure, and combustion-chamber length. The effects of these variables with the exception of combustion-chamber length will be discussed.

Combustion time. - The time for combustion to take place was estimated from a number of pressure-time diagrams for different engine conditions. The method by which the combustion time was determined from each pressure-time curve is shown in figure 4. Combustion time was considered to be the elapsed time between the beginning of combustion and the time at which peak pressure was reached. Measured values of combustion time varied from 0.003 to 0.009 second, with values in the region of 0.006 second predominating. Insufficient data were available to determine the combustion time as a function of the various engine and operating variables. The value of 0.006 second was therefore considered to be representative of the experimental data presented. All the combustion-chamber runs were made using 62-octane gasoline. No attempt was made to decrease combustion time by the use of more rapidly burning fuels.

In obtaining experimental data, combustion time was not investigated as a primary variable. The effects of combustion time on explosion-pressure ratio and over-all performance were therefore analytically studied. Combustion times of 0, 0.003, and 0.006 second were investigated in order to show the effect of decreasing combustion time below values experimentally obtained. Theoretical explosion-pressure ratio is shown in figure 5 as a function of fuel-air ratio for several combustion times and for three different ratios of exhaust-nozzle area to combustion-chamber cross-sectional area. The experimental data also presented in this figure will be discussed in the following section. The increase in performance that can be realized by decreasing combustion time is indicated in figure 5. As an example of the increase in explosion-pressure ratio that can be obtained by decreasing combustion time, figure 5(c) indicates that for a ratio of exhaust-nozzle area to combustion-chamber cross-sectional area of 1/6, decreasing the combustion time from the average measured value of 0.006 to 0.003 second increases the explosion-pressure ratio by approximately 37 percent over the range of fuel-air ratio studied. This change in explosion-pressure ratio represents an increase of from approximately 45 to more than 60 percent of the maximum possible explosion-pressure ratio with ideal constant-volume combustion (zero combustion time). Even greater increases in performance are shown in figures 5(a) and 5(b) for the larger ratios of exhaust-nozzle area to combustion-chamber cross-sectional area.

Fuel-air ratio. - The effects of fuel-air ratio on explosion-pressure ratio are shown in figure 5 for both calculated and experimentally determined data. The calculated explosion-pressure ratio continually increases with fuel-air ratio over the range investigated, which is entirely below stoichiometric fuel-air ratio. The experimental data, however, show an increase and then a decrease in explosion-pressure ratio with the peak occurring at a fuel-air ratio of approximately 0.04 in most cases. This peaking of the experimental data at fuel-air ratios less than stoichiometric is probably due to the fact that the experimentally determined fuel-air ratio is based on the over-all ratio of fuel flow to air flow. The possibility that varying amounts of fuel and air could escape from the combustion chamber during the charging process and the probable stratification of fuel in the chamber could result in a fuel-air ratio in most of the effective combustion zone that would be higher than indicated in figure 5.

Calculated explosion-pressure ratios for a combustion time of 0.006 second varied from approximately 1.7 to 5 depending upon the ratio of exhaust-nozzle area to combustion-chamber cross-sectional area and fuel-air ratio; the maximum value occurred at 0.065, which

is approximately stoichiometric fuel-air ratio. The maximum explosion-pressure ratio experimentally obtained was 2.9 at an over-all fuel-air ratio of approximately 0.04. Inasmuch as the experimentally determined explosion-pressure ratios decreased for richer or leaner fuel-air ratios, it is quite possible that stoichiometric fuel-air ratio existed in the combustion zone of the chamber when the over-all fuel-air ratio was only 0.04. A comparison of maximum calculated and maximum experimental explosion-pressure ratios indicates that in general the experimental values are considerably lower than the calculated values at a combustion time of 0.006 second. Several possible explanations exist for this apparent discrepancy between the measured and calculated values. The decrease in explosion-pressure ratio with an increase in cycle frequency from 15 to 30 cycles per second is probably due to a decrease in volumetric efficiency and to contamination of the fresh charge resulting from incomplete purging of the chamber and will be considered later in the discussion of cycle frequency. It was pointed out in the discussion of combustion time that insufficient data were available to determine combustion time as a function of engine and operating variables. The average measured value of combustion time used in the calculations may therefore not be representative over the entire range of fuel-air ratios.

Part of the difference between calculated and experimental explosion-pressure ratios is probably due to the incomplete utilization of the energy in the fuel. For the calculated quantities, combustion efficiency was assumed to be 100 percent. In the actual cycle, some unburned fuel may be expelled from the chamber during the charging process, some fuel may not be burned as a result of poor mixing, and part of the fuel may be burned during the blowdown process. All these factors reduce the amount of useful energy obtained from the fuel. Although it was impossible to determine the magnitude of each of these factors, it is believed that their combined effect is sufficiently large to reduce by an appreciable amount the percentage of the fuel that is fully utilized.

Ratio of exhaust-nozzle area to combustion-chamber cross-sectional area. - A cross plot of figure 5 presented in figure 6 shows the theoretical and experimental variation in explosion pressure with variation in the ratio of exhaust-nozzle area to combustion-chamber cross-sectional area A_e/A_b at a given fuel-air ratio. The calculated curve indicates, that, for a combustion time of 0.006 second and a fuel-air ratio of 0.04, decreasing the exhaust-nozzle area from 1/3 to 1/6 of the cross-sectional area of the combustion chamber will increase the explosion-pressure ratio from 1.8 to 3.8 or more than 100 percent. As can be seen from the experimental data in figure 6, however, only a small increase was realized for the

combustion chamber investigated. This increase was 2.6 to 2.8 and the explosion pressure appeared to be almost independent of exhaust-nozzle area. Reasons for not achieving experimentally the improvement in explosion pressure with decreasing exhaust-nozzle area predicted from theory are not readily apparent from the data. One factor that probably affected the results is combustion time. As previously noted, the experimental combustion time was generally about 0.006 second. When the experimental data were higher than the explosion-pressure data calculated for a combustion time of 0.006, the experimental combustion time was probably less than 0.006 second. If this supposition is true, the data indicate that combustion time was increased by decreasing the ratio of exhaust-nozzle area to combustion-chamber cross-sectional area.

Another factor that might prevent an increase in explosion-pressure ratio with a decrease in A_e/A_b at a given frequency is the fact that the time for purging or charging of the chamber relative to total cycle time was fixed by the inlet-valve design. An analysis of the cycle indicates that the time for purging should be increased as the nozzle area is decreased. It could therefore be reasoned that the time for purging, although adequate for the large exhaust nozzles, was too short for the smaller nozzle. This inadequate purging time would result in a dilution of the fresh charge and could lower combustion-pressure rise.

Cycle frequency. - A representative experimental curve of the change in explosion-pressure ratio with changes in cycle frequency is shown in figure 7. The rapid decrease in explosion-pressure ratio with increasing cycle frequency (from a value of 2.90 at 15 cps to 1.80 at 40 cps) is probably caused by a lower weight of air flow per cycle and poorer combustion at the higher frequencies. It was found in the investigation that as the cycle frequency increased the combustion process approached steady burning. For each of the exhaust nozzles investigated, there was some value of cycle frequency (this value increased as nozzle area increased), determined by the inlet pressure and fuel-air ratio, above which it was impossible to maintain intermittent combustion.

For a given inlet pressure and ratio of exhaust-nozzle area to combustion-chamber cross-sectional area, the cyclic flow to the combustion chamber decreased as the frequency increased. Figure 8 shows this change in weight flow on the basis of volumetric efficiency, defined here as the ratio of air supplied to the combustion chamber per cycle divided by the volume of the combustion chamber, over the same range of frequencies and for the same nozzle size presented in figure 7. This smaller mass of air results in less pressure rise during the combustion process, as has already be indicated in figure 7.

396

Inlet-pressure ratio. - Inlet-pressure ratio is defined as the ratio of the pressure at the inlet valve to ambient pressure. Experimentally determined explosion-pressure ratios are shown in figure 9 as a function of fuel-air ratio for three inlet-pressure ratios. An examination of this figure indicates that the explosion-pressure ratio increases with an increase in inlet-pressure ratio. At a fuel-air ratio of 0.04 and an A_e/A_b of 1/6, explosion-pressure ratio increased from 2.0 at an inlet-pressure ratio of 1.10 to 2.62 at an inlet-pressure ratio of 1.25.

Thrust and Specific Fuel Consumption

The jet thrust per pound of air handled per unit time and the fuel economy of the combustion chamber are shown in figures 10 and 11, respectively, for the calculated and experimental data.

Thrust. - Calculated and experimentally determined values of jet thrust per pound of air handled per unit time are shown in figure 10 for three ratios of exhaust-nozzle area to combustion-chamber cross-sectional area, and for two cycle frequencies. The theoretical calculations indicate that the amount of thrust per pound of air for a combustion time of 0.006 second (the experimentally determined average combustion time) would vary between 14 and 46 pounds per pound of air per second depending upon A_e/A_b and the fuel-air ratio, the highest value occurring at the smallest nozzle ratio (1/6) and stoichiometric fuel-air ratio (fig. 10(c)). Decreasing the combustion time to 0.003 second increased the thrust values to a range between 28 and 80 pounds per pound of air per second for the same range of fuel-air ratios and the same exhaust-nozzle areas. This change in thrust represents an increase in jet thrust of almost 100 percent. Maximum possible jet thrust for ideal constant-volume combustion (zero combustion time) ranged from 62 to 185 pounds per pound of air per second with the highest value at a fuel-air ratio of 0.065.

Experimentally determined values of jet thrust varied between 25 and 35 pounds per pound of air per second, depending on the ratio of exhaust-nozzle area to combustion-chamber cross-sectional area and fuel-air ratio. Of the three ratios of exhaust-nozzle area to combustion-chamber-cross-sectional area investigated, the best performance was obtained with the ratio of 1/4 (thrust of 34 lb/(lb air)(sec) at a fuel-air ratio of 0.045).

Specific fuel consumption. - Calculated and experimentally determined values of thrust specific fuel consumption for three ratios of exhaust-nozzle area to combustion-chamber cross-sectional

area at two cycle frequencies are presented over a range of fuel-air ratios in figure 11. For a combustion time of 0.006 second, calculated values of specific fuel consumption ranged from approximately 2.5 pounds of fuel per hour per pound of thrust at a fuel-air ratio of 0.02 to 5.0 pounds of fuel per hour per pound of thrust at a fuel-air ratio of 0.065 for an A_e/A_b of 1/6 (fig. 11(c)). As the nozzle area increased, the specific fuel consumption also increased so that for an area ratio of 1/3 (fig. 11(a)) and a fuel-air ratio of 0.065, calculated specific fuel consumption increased to more than 10 pounds of fuel per hour per pound of thrust. Decreasing the combustion time from 0.006 to 0.003 second would in all cases reduce the thrust specific fuel consumption by more than 50 percent. As an indication of the lower limit of the specific fuel consumption, a curve of specific fuel consumption for the ideal constant volume cycle (zero combustion time) is also included in figure 11. These values range from 1.13 to 1.35 depending on fuel-air ratio. Experimentally determined thrust specific fuel consumption ranged from 3.9 pounds of fuel per hour per pound of thrust at the low fuel-air ratios to approximately 9 pounds at the highest fuel-air ratio and largest exhaust nozzle investigated. Minimum fuel consumption occurred for an A_e/A_b of 1/4 and a fuel-air ratio of approximately 0.035 (fig. 11(b)).

Applications of Explosion-Cycle Combustion Chamber

One simple application of the combustion chamber described would be to a jet-propulsion engine consisting of an inlet diffuser and timed inlet valve, an explosion-cycle combustion chamber, and a fixed-area exit nozzle. The range of usefulness of such an engine could be determined by a comparison with the resonant pulse-jet and steady-flow ram-jet engines. The values of thrust per pound of air and specific fuel consumption reported can be compared with pulse-jet data presented in reference 4. The calculated values presented indicate that greater thrusts per pound of air than those obtained in the pulse-jet engine are obtainable at considerably lower specific fuel consumption. The experimental data presented, however, gave values of thrust per pound of air that were approximately only 50 percent of that obtained on the pulse jet and the minimum specific fuel consumption was also 20 percent greater than that obtained on the pulse-jet engine. These values indicate that on a theoretical basis this engine is capable of competing with the pulse-jet engine.

Because the explosion-cycle jet engine discussed herein can develop considerably higher thrusts than the ram jet at low velocities, it might therefore be used to supplement a ram-jet engine. At low flight

velocities, it would operate on the explosion cycle and take advantage of the increased thrust obtainable from this type of operation. At higher flight speeds, the inlet valve could be locked in an open position or discarded entirely and the unit would then operate as an ordinary ram jet. In this way, the high thrusts that can be obtained at high flight velocities by the ram jet would be utilized.

Another application of the explosion-cycle combustion chamber would be to a turbojet engine consisting of a compressor, explosion-cycle combustion chamber, turbine, and exhaust nozzle. An engine of this type would be somewhat similar to the Holzwarth turbine but would not be provided with combustion-chamber exhaust valves as in the Holzwarth turbine.

SUMMARY OF RESULTS

The following results were obtained from an analytical and experimental investigation of an explosion-cycle combustion chamber for a jet-propulsion engine.

1. For the configuration investigated, combustion time varied between 0.003 and 0.009 second with values in the vicinity of 0.006 being most predominant.

2. Explosion-pressure ratios calculated on the basis of a combustion time of 0.006 second ranged from approximately 1.7 to 5.0 depending upon the ratio of exhaust-nozzle area to combustion-chamber cross-sectional area A_e/A_b and fuel-air ratio with the highest value occurring at approximately stoichiometric fuel-air ratio. The highest explosion-pressure ratio obtained experimentally was 2.9 at an overall fuel-air ratio of approximately 0.04. Explosion-pressure ratio decreased for richer or leaner fuel-air ratios.

3. Calculations indicated that if the combustion time could be reduced from 0.006 to 0.003 second, explosion-pressure ratios could be increased by approximately 37 percent over the range of conditions investigated.

4. Theoretical calculations indicated that the explosion-pressure ratio varied with changes in the ratio of exhaust-nozzle area to combustion-chamber cross-sectional area. At a fuel-air ratio of 0.04, the calculations indicated that the explosion-pressure ratio could be increased from 1.8 to 3.8 by decreasing A_e/A_b from 1/3 to 1/6. Experimentally determined explosion-pressure ratios, however, were practically independent of changes in A_e/A_b , varying only from 2.6 to 2.8 over the same range of nozzle sizes.

5. Explosion-pressure ratios that were experimentally determined rapidly decreased with an increase in cycle frequency and increased with an increase in inlet-pressure ratio. At a fuel-air ratio of 0.04 and a ratio of exhaust-nozzle area to combustion-chamber cross-sectional area of 1/6, explosion-pressure ratio decreased from 2.90 at 15 cycles per second to 1.8 at 40 cycles per second. For the same fuel-air ratio and A_e/A_b , explosion-pressure ratio increased from 2.0 at an inlet-pressure ratio of 1.10 to 2.62 at an inlet-pressure ratio of 1.25.

6. Theoretical calculations indicated that the jet thrust for a combustion time of 0.006 second would vary from 14 to 46 pounds per pound of air per second with the highest value at a fuel-air ratio of 0.065 and the smallest ratio of exhaust-nozzle area to combustion-chamber cross-sectional area (A_e/A_b , 1/6). Measured values of thrust for the same range of conditions varied from 25 to 35 pounds per pound of air per second with the highest values occurring for an A_e/A_b of 1/4, and at an over-all fuel-air ratio of 0.045.

7. For a combustion time of 0.006 second, calculated values of specific fuel consumption varied from 2.5 pounds of fuel per hour per pound of thrust to more than 10 pounds, depending upon the fuel-air ratio and nozzle size. Experimental values of thrust specific fuel consumption ranged from approximately 4 to 9 pounds per hour over the same range of conditions, with the minimum value occurring at an A_e/A_b of 1/4 and an over-all fuel-air ratio of 0.035.

8. Calculated values indicated that reducing the combustion time from 0.006 to 0.003 second would result in an increase of jet thrust of approximately 100 percent and a reduction in specific fuel consumption of more than 50 percent over the range of conditions investigated.

Flight Propulsion Research Laboratory,
National Advisory Committee for Aeronautics,
Cleveland, Ohio, June 4, 1948.

APPENDIX A

SYMBOLS

- A_b cross-sectional area of combustion chamber, (sq ft)
 A_e area of exhaust nozzle, (sq ft)
 c_p specific heat at constant pressure, (Btu/(lb)(°F))
 c_v specific heat at constant volume, (Btu/(lb)(°F))
 F jet thrust, (lb)
 f/a fuel-air ratio
 g acceleration of gravity, (ft/sec²)
 h heating value of fuel, (Btu/lb)
 I total impulse, (lb-sec)
 I_B impulse during blowdown, (lb-sec)
 I_p impulse during purging, (lb-sec)
 J mechanical equivalent of heat, (ft-lb/Btu)
 L combustion-chamber length, (ft)
 M mass flow of gas out of combustion chamber at any instant, (slugs/sec)
 m mass of gas in combustion chamber at any instant, (slugs)
 n cycle frequency
 P pressure in combustion chamber at any instant, (lb/sq ft)
 P_0 ambient pressure, (lb/sq ft)
 R gas constant, (ft-lb/(lb)(°R))
 T temperature of gas in combustion chamber at any instant, (°R)
 T_0 ambient temperature, (°R)
 t time, (sec)

t_B	blowdown time, (sec)
t_c	combustion time, (sec)
t_n	cycle time, (sec)
t_p	purging time, (sec)
U	jet velocity, (ft/sec)
U_B	jet velocity during blowdown, (ft/sec)
U_p	jet velocity during purging, (ft/sec)
V	volume of combustion chamber, (cu ft)
v	specific volume of gases in combustion chamber at any instant (cu ft slug)
W_a	weight of air, (lb/cycle)
W_f	weight of fuel, (lb/cycle)
γ	ratio of specific heats
ρ	density of gas in combustion chamber at any instant, (slugs/cu ft)

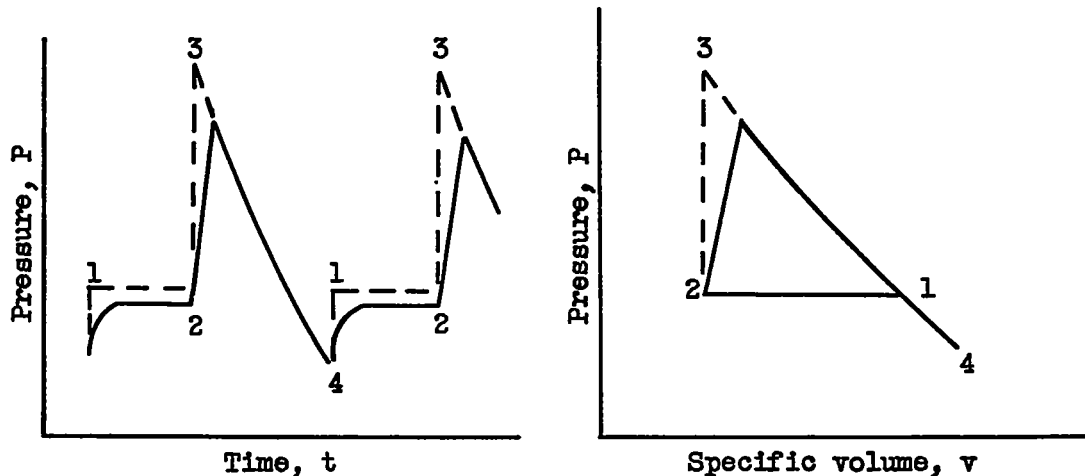
Subscripts:

- 1 beginning of charging or purging period
- 2 end of charging or purging period
- 3 end of combustion process
- 4 end of blowdown period
- cr critical
- e exhaust-nozzle throat

APPENDIX B

ANALYSIS OF CYCLE

The cycle upon which the analysis is based is illustrated in the following diagrams:



In both diagrams, the actual cycle is shown by the solid line and the ideal explosion cycle by the dashed line. The sequence of operation is as follows: Blowdown from the maximum conditions of temperature and pressure to atmospheric pressure occurs from points 3 to 4; at point 4 the inlet valve opens and the residual gases are then compressed from points 4 to 1 by the inlet pressure; charging and purging occur simultaneously at constant pressure from points 1 to 2, and the cycle is completed with combustion from points 2 to 3.

Explosion-Pressure Ratio

Explosion-pressure and temperature ratios were obtained in the following manner. The general energy equation for any combustion process can be written in the following form (reference 5).

$$W(E_{m,2} - E_{m,1}) + \frac{WE}{J} + Q + W E_T = W_F h \quad (1a)$$

where

W weight of mixture, lb

$E_{m,1}$ molecular energy of mixture before combustion, Btu/lb mixture

$E_{m,2}$ molecular energy of mixture after combustion, Btu/lb mixture

E mechanical energy departing from system, ft-lb/lb mixture

Q energy emitted from system as heat during combustion, Btu

E_r residual energy in mixture due to incomplete combustion of fuel,
Btu/lb mixture

The other symbols are defined in appendix A.

If the following assumptions are made

- (1) complete combustion
- (2) no heat loss during combustion process
- (3) change in molecular energy equal to change in internal energy
- (4) constant specific heat during combustion
- (5) volumetric efficiency of chamber equal to 100 percent

equation (la) can be written

$$W c_v \Delta T + \frac{WE}{J} = W_f h$$

or in differential form

$$W c_v \frac{dT}{dt} + \frac{W}{J} \frac{dE}{dt} = h \frac{dW_f}{dt} \quad (lb)$$

If the following substitutions are made in equation (lb)

$$c_v = \frac{R}{(\gamma-1)J}$$

$$W = W_a (1 + f/a)$$

$$dE = P \frac{dv}{g}$$

$$\frac{P}{g} \frac{dv}{dt} = \frac{RT}{v} \frac{dv}{dt}$$

and it is assumed that the fuel is consumed at a constant rate

$$\frac{dW_f}{dt} = \frac{W_f}{t_c}$$

then equation (1b) can be written

$$\frac{dT}{dt} + (\gamma - 1) \frac{T}{V} \frac{dv}{dt} = \frac{J}{R} (\gamma - 1) \frac{f/a}{f/a + 1} \frac{h}{t_c} \quad (1c)$$

296

A more convenient form for equation (1c) can be obtained by dividing by T_2 ; then

$$\frac{dT/T_2}{dt} + (\gamma - 1) \left(\frac{T}{T_2} \right) \frac{1}{V} \frac{dv}{dt} = \frac{J}{RT_0} (\gamma - 1) \left(\frac{T_0}{T_2} \right) \left(\frac{f/a}{f/a + 1} \right) \frac{h}{t_c} \quad (1d)$$

The change in specific volume of the gas can be determined from the following equations:

$$dv = d\left(\frac{V}{m}\right) = V \frac{dm}{m^2}$$

If $m = \rho V$ and $dm = \rho_e A_e U_B dt$

then

$$\frac{dv}{dt} = \frac{A_e U_B}{m} \left(\frac{\rho_e}{\rho} \right)$$

The change in specific volume during the combustion period can be most readily determined by assuming that critical conditions exist at the nozzle throat for the entire combustion process. During the actual combustion process, the pressure at the exhaust nozzle of the chamber will rise from ambient to critical. The assumption that critical conditions exist for the entire period will therefore tend to give conservative values of explosion-temperature and pressure ratio. For critical pressure at the nozzle throat

$$U_B = \left(\frac{2\gamma g RT}{\gamma + 1} \right)^{1/2}$$

and

$$\frac{\rho_e}{\rho} = \left(\frac{2}{\gamma + 1} \right)^{\frac{1}{\gamma-1}}$$

The change in specific volume with respect to time divided by the specific volume can now be written

$$\frac{1}{v} \frac{dv}{dt} = \frac{A_e}{A_b} \frac{1}{L} \left(\frac{2}{\gamma + 1} \right)^{\frac{1}{\gamma-1}} \left(\frac{T}{T_2} \right)^{1/2} \left(\frac{T_2}{T_0} \right)^{1/2} \left(\frac{2\gamma gRT_0}{\gamma + 1} \right)^{1/2} \quad (2)$$

The general energy equation for the combustion process can now be written

$$\frac{d\left(\frac{T}{T_2}\right)}{dt} = \frac{J}{RT_0} (\gamma - 1) \left(\frac{T_0}{T_2} \right) \left(\frac{f/a}{f/a + 1} \right) \frac{h}{t_c} - (\gamma - 1) \left(\frac{A_e}{A_b} \right) \left(\frac{1}{L} \right) \left(\frac{2\gamma gRT_0}{\gamma + 1} \right)^{1/2} \left(\frac{T}{T_2} \right)^{3/2} \left(\frac{T_2}{T_0} \right)^{1/2} \left(\frac{2}{\gamma + 1} \right)^{\frac{1}{\gamma-1}} \quad (3a)$$

or

$$\int_1^{T_3/T_2} \frac{d\left(\frac{T}{T_2}\right)}{\frac{J}{RT_0} (\gamma - 1) \left(\frac{T_0}{T_2} \right) \left(\frac{f/a}{f/a + 1} \right) \left(\frac{h}{t_c} \right) - (\gamma - 1) \left(\frac{A_e}{A_b} \right) \left(\frac{1}{L} \right) \left(\frac{2\gamma gRT_0}{\gamma + 1} \right)^{1/2} \left(\frac{T}{T_2} \right)^{3/2} \left(\frac{T_2}{T_0} \right)^{1/2} \left(\frac{2}{\gamma + 1} \right)^{\frac{1}{\gamma-1}}} dt = t_c \quad (3b)$$

Equation (3b) was integrated graphically in order to obtain the temperature ratio developed during the combustion process. In the evaluation of equation (3b), those quantities that do not vary with time can be grouped together to give the following equation

$$\int_1^{T_3/T_2} \frac{d\left(\frac{T}{T_2}\right)}{A - B \left(\frac{T}{T_2}\right)^{3/2}} = t_c$$

where

$$A = (\gamma-1) \left(\frac{J}{RT_0} \right) \left(\frac{f/a}{f/a + 1} \right) \left(\frac{h}{t_c} \right) \left(\frac{T_0}{T_2} \right)$$

and

$$B = (\gamma-1) \left(\frac{A_e}{A_b} \right) \left(\frac{l}{L} \right) \left(\frac{2\gamma gRT_0}{\gamma + 1} \right)^{1/2} \left(\frac{2}{\gamma + 1} \right)^{\frac{1}{\gamma-1}} \left(\frac{T_2}{T_0} \right)^{1/2}$$

From the general gas law it can be shown that

$$\frac{dv}{v} + \frac{dp}{P} = \frac{dT}{T}$$

If dv is replaced by its equivalent value given in equation (2), then

$$\frac{dp}{P} = \frac{dT}{T} - \left(\frac{A_e}{A_b} \right) \left(\frac{l}{L} \right) \left(\frac{2\gamma gRT_0}{\gamma + 1} \right)^{1/2} \left(\frac{T}{T_2} \right)^{1/2} \left(\frac{T_2}{T_0} \right)^{1/2} \left(\frac{2}{\gamma + 1} \right)^{\frac{1}{\gamma-1}} dt$$

And if dt is replaced by its equivalent value given in equation (3a), the preceding equation can be written

$$\frac{dp}{P} = \frac{dT}{T} - \frac{\left(\frac{1}{\gamma - 1}\right) \left(\frac{T}{T_2}\right)^{1/2} d\left(\frac{T}{T_2}\right)}{\left[\frac{J}{RT_0} \left(\frac{T_0}{T_2}\right) \left(\frac{r/a}{r/a + 1}\right) \left(\frac{h}{t_0}\right) \right.} \\ \left. \left[\left(\frac{A_e}{A_b}\right) \left(\frac{1}{L}\right) \left(\frac{2\gamma g RT_0}{\gamma + 1}\right)^{1/2} \left(\frac{T_2}{T_0}\right)^{1/2} \left(\frac{2}{\gamma + 1}\right)^{1/2} \right] - \left(\frac{T}{T_2}\right)^{3/2}} \quad (4)$$

When equation (4) is integrated

$$\log_e\left(\frac{P_3}{P_2}\right) = \log_e\left(\frac{T_3}{T_2}\right) - \int_1^{T_3/T_2} \frac{\left(\frac{1}{\gamma - 1}\right) \left(\frac{T}{T_2}\right)^{1/2} d\left(\frac{T}{T_2}\right)}{\left(\frac{A_b}{A_e}\right) \left(L\right) \left(\frac{r/a}{r/a + 1}\right) \left(\frac{h}{t_0}\right) \left(\frac{J}{RT_0}\right) \left(\frac{T_0}{T_2}\right)^{3/2} \left(\frac{\gamma + 1}{2}\right)^{1/2} \left(\frac{1}{\gamma g RT_0}\right)^{1/2} - \left(\frac{T}{T_2}\right)^{3/2}} \quad (5)$$

$$\log_e\left(\frac{P_3}{P_2}\right) = \log_e\left(\frac{T_3}{T_2}\right) - \frac{1}{\gamma - 1} \int_1^{T_3/T_2} \frac{\left(\frac{T}{T_2}\right)^{1/2} d\left(\frac{T}{T_2}\right)}{\frac{A}{B} - \left(\frac{T}{T_2}\right)^{3/2}}$$

Equation (5) can be most readily evaluated by graphical integration to give the explosion pressure developed during the combustion process.

The explosion-pressure ratio for ideal constant-volume combustion can be obtained if it is assumed that combustion time is instantaneous. Equation (5) then reduces to

$$\log_e \left(\frac{P_3}{P_2} \right) = \log_e \left(\frac{T_3}{T_2} \right)$$

and

$$\frac{P_3}{P_2} = \frac{T_3}{T_2}$$

Explosion-temperature ratio can be calculated from the following equation if the heat required to raise the temperature of the fuel to the final temperature of the mixture is neglected:

$$W_a c_v (T_3 - T_2) = h W_f$$

$$c_v T_2 \left(\frac{T_3}{T_2} \right)^{-1} = h f/a$$

$$\frac{T_3}{T_2} = \frac{h f/a}{c_v T_0 \left(\frac{T_2}{T_0} \right)} + 1$$

and

$$\frac{R}{J} = c_p - c_v = (\gamma - 1) c_v$$

then

$$\frac{T_3}{T_2} = \frac{h f/a J (\gamma - 1)}{R T_0 \left(\frac{T_2}{T_0} \right)} + 1$$

Thrust

The thrust output can be obtained from a consideration of the impulse during the blowdown and charging periods. If the mass flow out of the combustion chamber at any instant is equal to M , and if it is assumed that the theoretically correct nozzle is used, then the instantaneous jet thrust during blowdown is equal to

$$F = M U_B$$

The outflow from the chamber is equal to the rate of change in the total mass of gas in the chamber with respect to time.

$$M = \frac{dm}{dt}$$

and

$$F = U_B \frac{dm}{dt}$$

The total impulse during the blowdown period is equal to

$$I_B = \int F dt = \int U_B dm \quad (6)$$

The mass of gas in the chamber at any instant is equal to

$$m = \rho V$$

and from the adiabatic relation

$$m = m_3 \left(\frac{P}{P_3} \right)^{\frac{1}{\gamma}}$$

Differentiating the preceding equation with respect to pressure ratio gives

$$dm = \frac{1}{\gamma} m_3 \left(\frac{P}{P_3} \right)^{\frac{1-\gamma}{\gamma}} d\left(\frac{P}{P_3} \right) \quad (7)$$

The jet velocity can be written as

$$\begin{aligned} U_B &= (2 g J)^{1/2} \left\{ c_p T \left[1 - \left(\frac{P_0}{P} \right)^{\frac{\gamma-1}{\gamma}} \right]^{1/2} \right\} \\ &= (2 g J c_p T_3)^{1/2} \left[\left(\frac{P}{P_3} \right)^{\frac{\gamma-1}{\gamma}} - \left(\frac{P_0}{P_3} \right)^{\frac{\gamma-1}{\gamma}} \right]^{1/2} \end{aligned} \quad (8)$$

Equation (6) can now be written

$$I_B = \frac{m_3}{\gamma} (2 g J c_p T_3)^{1/2} \left\{ \int \left(\frac{P}{P_3} \right)^{\frac{1-\gamma}{\gamma}} \left[\left(\frac{P}{P_3} \right)^{\frac{\gamma-1}{\gamma}} - \left(\frac{P_0}{P_3} \right)^{\frac{\gamma-1}{\gamma}} \right]^{1/2} d \left(\frac{P}{P_3} \right) \right\} \quad (9)$$

Equation (9) is more useful in the following form:

$$I_B = \frac{P_0 V}{\sqrt{\gamma g R T_0}} \left(\frac{2}{\gamma - 1} \right)^{1/2} \left(\frac{P_3}{P_2} \right) \left(\frac{P_2}{P_0} \right) \left(\frac{T_2}{T_3} \right)^{1/2} \left(\frac{T_0}{T_2} \right)^{1/2} \left\{ \int_{P_0/P_3}^1 \left(\frac{P}{P_3} \right)^{\frac{1-\gamma}{\gamma}} \left[\left(\frac{P}{P_3} \right)^{\frac{\gamma-1}{\gamma}} - \left(\frac{P_0}{P_3} \right)^{\frac{\gamma-1}{\gamma}} \right]^{1/2} d \left(\frac{P}{P_3} \right) \right\} \quad (10)$$

Total impulse during blowdown was calculated by graphically integrating equation (10).

The impulse during the purging period is equal to

$$I_p = \int F dt$$

and the instantaneous jet thrust equals

$$F = U_p \frac{dm}{dt}$$

If it is assumed that the exhaust gases are purged at constant pressure and without mixing with the fresh charge, the velocity of the exhaust gas during purging is constant and is equal to

$$U_p = (2 g J c_p T_1)^{1/2} \left[1 - \left(\frac{P_0}{P_2} \right)^{\frac{\gamma-1}{\gamma}} \right]^{1/2}$$

The quantity of exhaust gas expelled from the chamber during the purging period is equal to

$$\text{dm} = m_4 = \frac{V P_0}{g R T_4}$$

The impulse during purging is now equal to

$$I_p = \frac{P_0 V}{g R T_4} (2 g J c_p T_1)^{1/2} \left[1 - \frac{P_0}{P_2} \frac{\gamma-1}{\gamma} \right]^{1/2} \quad (\text{lla})$$

Equation (lla) can be written in the following form

$$I_p = \frac{P_0 V \gamma}{\sqrt{\gamma g R T_0}} \left(\frac{2}{\gamma-1} \right)^{1/2} \left(\frac{T_0}{T_2} \right)^{1/2} \left(\frac{P_2}{P_0} \right)^{\frac{\gamma-1}{2\gamma}} \left[\left(\frac{P_2}{P_0} \right)^{\frac{\gamma-1}{\gamma}} - 1 \right]^{1/2} \quad (\text{llb})$$

The sum of the impulses during the blowdown and purging periods will be considered as the total impulse for the cycle. Total impulse therefore equals the sum of equations (10) and (llb)

$$I = I_B + I_p$$

the average thrust for the cycle will equal

$$F = \frac{I}{t_n} = nI$$

and the weight of air flow per unit time equals

$$W_a = n V \rho_2 g$$

By use of the general gas law

$$\begin{aligned} W_a &= \frac{n V P_2 g}{g R T_2} \\ &= \frac{n V g \gamma P_0}{\gamma g R T_0} \left(\frac{P_2}{P_0} \right) \left(\frac{T_0}{T_2} \right) \end{aligned}$$

Thrust per pound of air per unit time is equal to

$$\frac{F}{W_a} = \frac{\sqrt{\gamma g R T_0}}{\gamma g} \left(\frac{2}{\gamma - 1} \right)^{1/2} \left(\frac{T_2}{T_0} \right)^{1/2} \left(\frac{T_2}{T_3} \right)^{1/2} \left(\frac{P_3}{P_2} \right) \left\{ \int_{P_0/P_3}^1 \left(\frac{P}{P_3} \right)^{\frac{1-\gamma}{\gamma}} \left[\left(\frac{P}{P_3} \right)^{\frac{\gamma-1}{\gamma}} - \left(\frac{P_0}{P_3} \right)^{\frac{\gamma-1}{\gamma}} \right]^{1/2} d \left(\frac{P}{P_3} \right) \right. \\ \left. + \gamma \left(\frac{P_0}{P_3} \right)^{\frac{\gamma+1}{2\gamma}} \left[\left(\frac{P_2}{P_0} \right)^{\frac{\gamma-1}{\gamma}} - 1 \right]^{1/2} \right\}$$

The thrust specific fuel consumption is equal to

$$tsfc = \frac{3600 f/a}{F/W_a}$$

Cycle Time

The total time for one cycle is equal to the sum of the combustion, blowdown, and purging or charging times. The blowdown time is the sum of the time required to blowdown from maximum to critical temperature and pressure, plus the time required to blowdown from critical pressure to atmospheric pressure.

The change in the mass of exhaust gas in the combustion chamber can be written in the following form:

$$dm = \rho_e A_e U_B dt$$

(12a)

When pressure and temperature in the chamber are above the critical values, the following relations hold

$$U_B = \sqrt{\frac{\gamma P_e}{\rho_e}}$$

$$\frac{P_e}{P} = \left(\frac{2}{\gamma + 1}\right)^{\frac{\gamma}{\gamma-1}}$$

$$\frac{P_e}{\rho} = \left(\frac{2}{\gamma + 1}\right)^{\frac{1}{\gamma-1}}$$

By substituting the preceding expressions in equation (12a) the following equation is obtained:

$$dm = A_e \left(\frac{2}{\gamma + 1}\right)^{\frac{\gamma+1}{2(\gamma-1)}} \sqrt{\gamma P \rho} dt \quad (12b)$$

By using the adiabatic relation between pressure and density, equation (12b) can be written

$$dm = A_e \left(\frac{2}{\gamma + 1}\right)^{\frac{\gamma+1}{2(\gamma-1)}} (\gamma)^{1/2} \left[\rho_3 \left(\frac{P}{P_3}\right)^{1/\gamma} \left(\frac{P}{P_3}\right) P_3 \right]^{1/2} dt$$

$$dm = A_e \left(\frac{2}{\gamma + 1}\right)^{\frac{\gamma+1}{2(\gamma-1)}} (\gamma P_3 \rho_3)^{1/2} \left[\left(\frac{P}{P_3}\right)^{\frac{1+\gamma}{2\gamma}} \right] dt \quad (12c)$$

It has already been shown (equation (7)) that the change in mass is equal to

$$dm = \frac{1}{\gamma} m_3 \left(\frac{P}{P_3}\right)^{\frac{1-\gamma}{\gamma}} d\left(\frac{P}{P_3}\right)$$

When equations (7) and (12c) are equated

$$dt = \frac{m_3}{A_e} \left(\frac{\gamma + 1}{2} \right)^{\frac{\gamma + 1}{2(\gamma-1)}} \frac{1}{\gamma(\gamma P_3 P_3)^{1/2}} \left(\frac{P}{P_3} \right)^{\frac{1-3\gamma}{2\gamma}} d\left(\frac{P}{P_3} \right) \quad (13)$$

Equation (13) can be written in the following more convenient form:

$$dt = \left(\frac{A_b}{A_e} \right) (L) \left(\frac{\gamma + 1}{2} \right)^{\frac{\gamma + 1}{2(\gamma-1)}} \frac{1}{\gamma(\gamma g R T_0)^{1/2}} \left(\frac{T_0}{T_3} \right)^{1/2} \left(\frac{P}{P_3} \right)^{\frac{1-3\gamma}{2\gamma}} d\left(\frac{P}{P_3} \right)$$

Integrating gives

$$t_{3-cr} = \left(\frac{A_b}{A_e} \right) (L) \left(\frac{\gamma + 1}{2} \right)^{\frac{\gamma + 1}{2(\gamma-1)}} \frac{1}{\gamma(\gamma g R T_0)^{1/2}} \left(\frac{T_0}{T_3} \right)^{1/2} \int_{P_{cr}/P_3}^1 \left(\frac{P}{P_3} \right)^{\frac{1-3\gamma}{2\gamma}} d\left(\frac{P}{P_3} \right) \quad (14a)$$

$$= \left(\frac{A_b}{A_e} \right) (L) \left(\frac{\gamma + 1}{2} \right)^{\frac{\gamma + 1}{2(\gamma-1)}} \frac{1}{\gamma(\gamma g R T_0)^{1/2}} \left(\frac{T_0}{T_3} \right)^{1/2} \frac{2\gamma}{1-\gamma} \left[1 - \left(\frac{P_{cr}}{P_3} \right)^{\frac{1-\gamma}{2\gamma}} \right] \quad (14b)$$

Critical pressure in the chamber can be related to atmospheric pressure by the following equation: 51

$$P_{\text{cr}} = P_0 \left(\frac{\gamma + 1}{2} \right)^{\frac{\gamma}{\gamma - 1}}$$

Rewriting equation (14b) gives

$$t_{3-\text{cr}} = \left(\frac{A_p}{A_e} \right) \frac{L}{(\gamma g R T_0)^{1/2}} \left(\frac{\gamma + 1}{2} \right)^{\frac{\gamma + 1}{2(\gamma - 1)}} \left(\frac{T_0}{T_3} \right)^{1/2} \frac{2}{\gamma - 1} \left[\left(\frac{P_0}{P_3} \right)^{\frac{1-\gamma}{2\gamma}} \left(\frac{2}{\gamma + 1} \right)^{1/2} - 1 \right] \quad (14c)$$

Equation (14c) can be used to calculate the time required to blowdown from maximum pressure to critical pressure.

The time to blowdown from critical to atmospheric pressure can be determined in the following manner: For flow below critical pressure, the change in mass (equations (8) and (12a)) is equal to

$$dm = \rho_e A_e (2gJ_{\rho} T_{\text{cr}})^{1/2} \left[\left(\frac{P}{P_{\text{cr}}} \right)^{\frac{\gamma-1}{\gamma}} - \left(\frac{P_0}{P_{\text{cr}}} \right)^{\frac{\gamma-1}{\gamma}} \right]^{1/2} dt \quad (15a)$$

For flow below critical, the following relations hold:

$$\rho_e = \rho_3 \left(\frac{P_0}{P_3} \right)^{1/\gamma} = \frac{P_3}{g R T_3} \left(\frac{P_0}{P_3} \right)^{1/\gamma}$$

$$T_{\text{cr}} = T_3 \left(\frac{\gamma + 1}{2} \right) \left(\frac{P_0}{P_3} \right)^{\frac{\gamma-1}{\gamma}}$$

When these relations are substituted in equation (15a), the following equation is obtained:

$$dm = A_e \left(\frac{P_3}{P_0} \right)^{\frac{\gamma-1}{2\gamma}} \left(\frac{T_0}{T_3} \right)^{1/2} \gamma \left(\frac{2}{\gamma-1} \right)^{1/2} \frac{P_0}{\sqrt{\gamma gRT_0}} \left[\left(\frac{P}{P_0} \right)^{\frac{\gamma-1}{\gamma}} - 1 \right]^{1/2} dt \quad (15b)$$

Equation (7) can be rewritten for subcritical flow as

$$dm = \frac{1}{\gamma} m_{or} \left(\frac{P}{P_{or}} \right)^{\frac{1-\gamma}{\gamma}} d\left(\frac{P}{P_{or}} \right) \quad (16a)$$

Equation (16a) can be rewritten in the following form:

$$dm = \frac{P_0 V}{\gamma gRT_0} \left(\frac{T_0}{T_3} \right) \left(\frac{P_3}{P_0} \right)^{\frac{\gamma-1}{\gamma}} \left(\frac{P}{P_0} \right)^{\frac{1-\gamma}{\gamma}} d\left(\frac{P}{P_0} \right) \quad (16b)$$

Equating equations (15b) and (16b) gives

$$dt = \left(\frac{A_b}{A_e} \right) \frac{L}{\sqrt{\gamma gRT_0}} \left(\frac{T_0}{T_3} \right)^{1/2} \left(\frac{P_3}{P_0} \right)^{\frac{\gamma-1}{2\gamma}} \left(\frac{\gamma-1}{2} \right)^{1/2} \frac{1}{\gamma} \left(\frac{P}{P_0} \right)^{\frac{1-\gamma}{\gamma}} \left[\left(\frac{P}{P_0} \right)^{\frac{\gamma-1}{\gamma}} - 1 \right]^{1/2} d\left(\frac{P}{P_0} \right)$$

Integrating gives

$$t_{cr-4} = \left(\frac{A_p}{A_e} \right) \frac{L}{\sqrt{\gamma g R T_0}} \left(\frac{T_0}{T_3} \right)^{1/2} \left(\frac{P_3}{P_0} \right)^{\frac{\gamma-1}{2\gamma}} \left(\frac{\gamma-1}{2} \right)^{1/2} \frac{1}{\gamma} \int_1^{\frac{(\gamma+1)}{2}^{\frac{\gamma}{\gamma-1}}} \frac{\left(\frac{P}{P_0} \right)^{\frac{1-\gamma}{\gamma}} d\left(\frac{P}{P_0} \right)}{\left[\left(\frac{P}{P_0} \right)^{\frac{\gamma-1}{\gamma}} - 1 \right]^{1/2}} \quad (17)$$

The integral of equation (17) can be very readily evaluated by graphical integration. The blowdown time t_B is equal to the sum of t_{3-cr} and t_{cr-4} .

Time required to purge the combustion chamber may be calculated by considering the gas remaining in the chamber at the end of the blowdown period

$$m_4 = \frac{V P_0}{g R T_4} \quad (18)$$

$$= \rho_e A_e U_p t_p \quad (19)$$

By equating equations (18) and (19) and using the gas laws, the following equation can be obtained:

$$t_p = \left(\frac{A_p}{A_e} \right) \frac{L}{\sqrt{\gamma g R T_0}} \left(\frac{T_0}{T_3} \right)^{1/2} \left(\frac{P_3}{P_0} \right)^{\frac{\gamma-1}{2\gamma}} \left(\frac{\gamma-1}{2} \right)^{1/2} \left[\left(\frac{P_2}{P_0} \right)^{\frac{\gamma-1}{\gamma}} - 1 \right]^{-1/2}$$

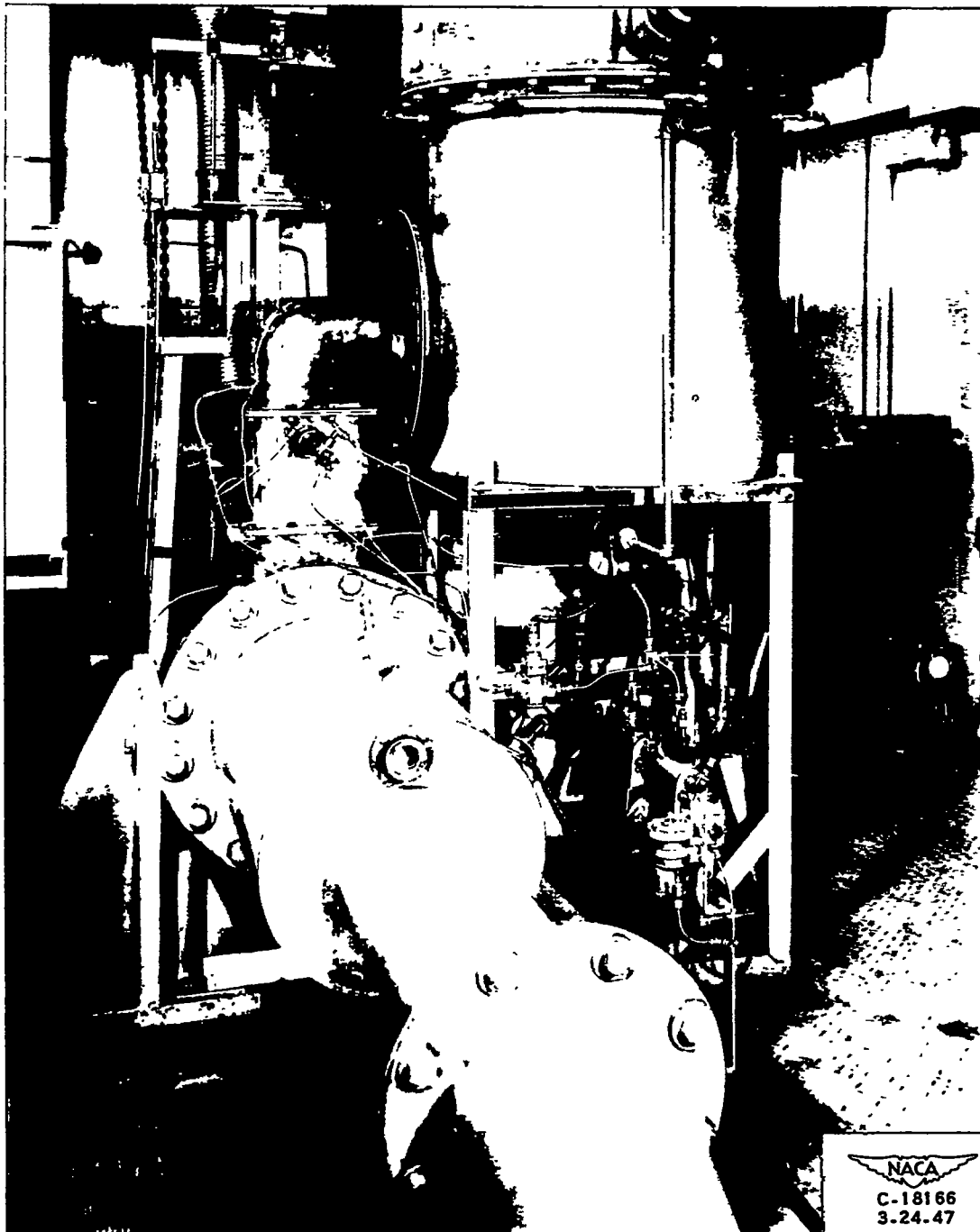
If t_c is the time during which combustion occurs, then the total cycle time is equal to

$$t_n = \left(\frac{A_p}{A_e} \right) \frac{L}{\sqrt{\gamma g R T_0}} \left(\frac{T_0}{T_3} \right)^{1/2} \left(\frac{P_3}{P_0} \right)^{\frac{\gamma-1}{2\gamma}} \left(\frac{\gamma+1}{2} \right)^{1/2} \left\{ \left(\frac{\gamma+1}{2} \right)^{\frac{1}{\gamma-1}} \left(\frac{2}{\gamma-1} \right)^{3/2} \left[1 - \left(\frac{P_0}{P_3} \right)^{\frac{\gamma-1}{2\gamma}} \left(\frac{\gamma+1}{2} \right)^{1/2} \right] \right. \\ \left. + \frac{1}{\gamma} \int_1^{\left(\frac{\gamma+1}{2} \right)^{\frac{\gamma}{\gamma-1}}} \frac{d \left(\frac{P}{P_0} \right)}{\left(\frac{P}{P_0} \right)^{\frac{\gamma-1}{\gamma}} \left[\left(\frac{P}{P_0} \right)^{\frac{\gamma-1}{\gamma}} - 1 \right]^{1/2}} + \left[\left(\frac{P_2}{P_0} \right)^{\frac{\gamma-1}{\gamma}} - 1 \right]^{1/2} \right\} + t_c$$

REFERENCES

1. Stodola, A.: *The Gas Turbine. Steam and Gas Turbines*, vol. II, chap. XI. Peter Smith (New York), 1945, p. 1250.
2. Edelman, L. B.: *The Pulsating Jet Engine - Its Evolution and Future Prospects*. SAE Quarterly Trans., vol. 1, no. 2, April 1947, pp. 204-216.
3. Pinkel, Benjamin, Turner, L. Richard, Voss, Fred, and Humble, Leroy V.: *Exhaust-Stack Nozzle Area and Shape for Individual Cylinder Exhaust-Gas Jet-Propulsion System*. NACA Rep. No. 765, 1943.
4. Manganiello, Eugene J., Valerino, Michael F., and Essig, Robert H.: *Sea-Level Performance Tests of 22-Inch-Diameter Pulse-Jet Engine at Various Simulated Ram Pressures*. NACA MR No. E5J02, 1945.
5. Kiefer, Paul J., and Stuart, Milton C.: *Combustion. Principles of Engineering Thermodynamics*, ch. XV. John Wiley & Sons, Inc., 1930, p. 411.

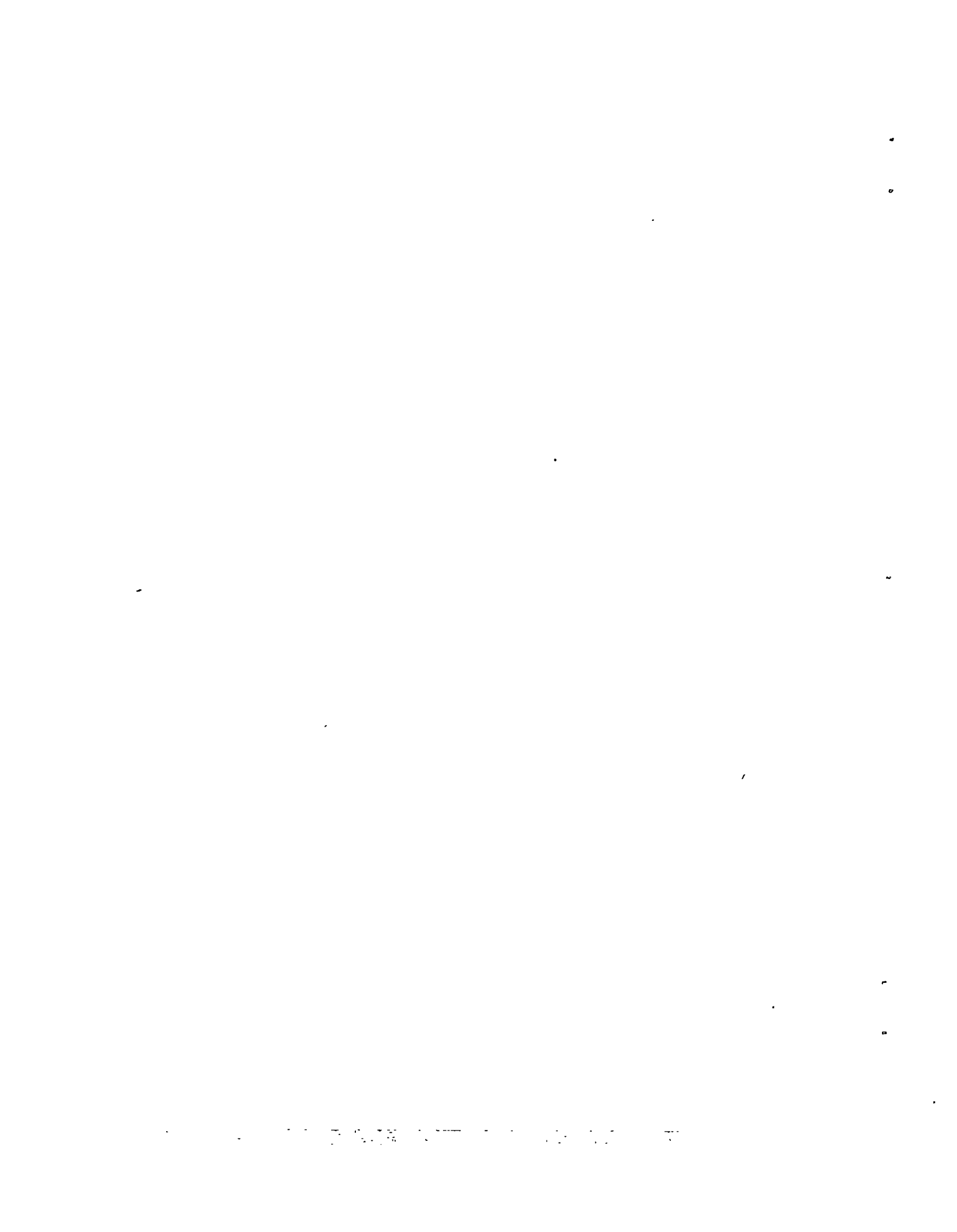
963



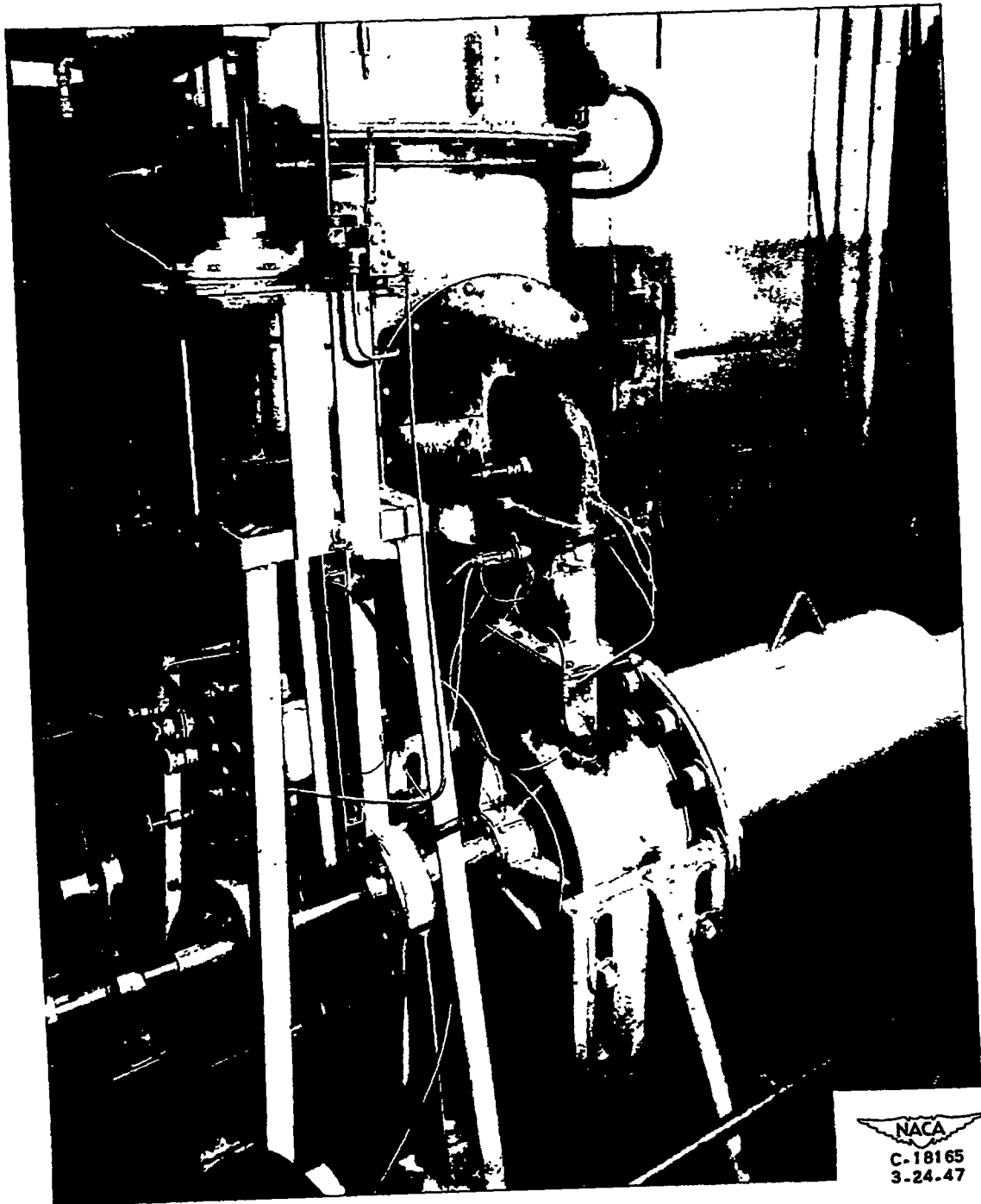
NACA
C-18166
3.24.47

(a) Front view.

Figure 1. - Setup of explosion-cycle combustion chamber.



965



NACA
C-18165
3-24-47

(b) Side view.

Figure 1. - Concluded. Setup of explosion-cycle combustion chamber.



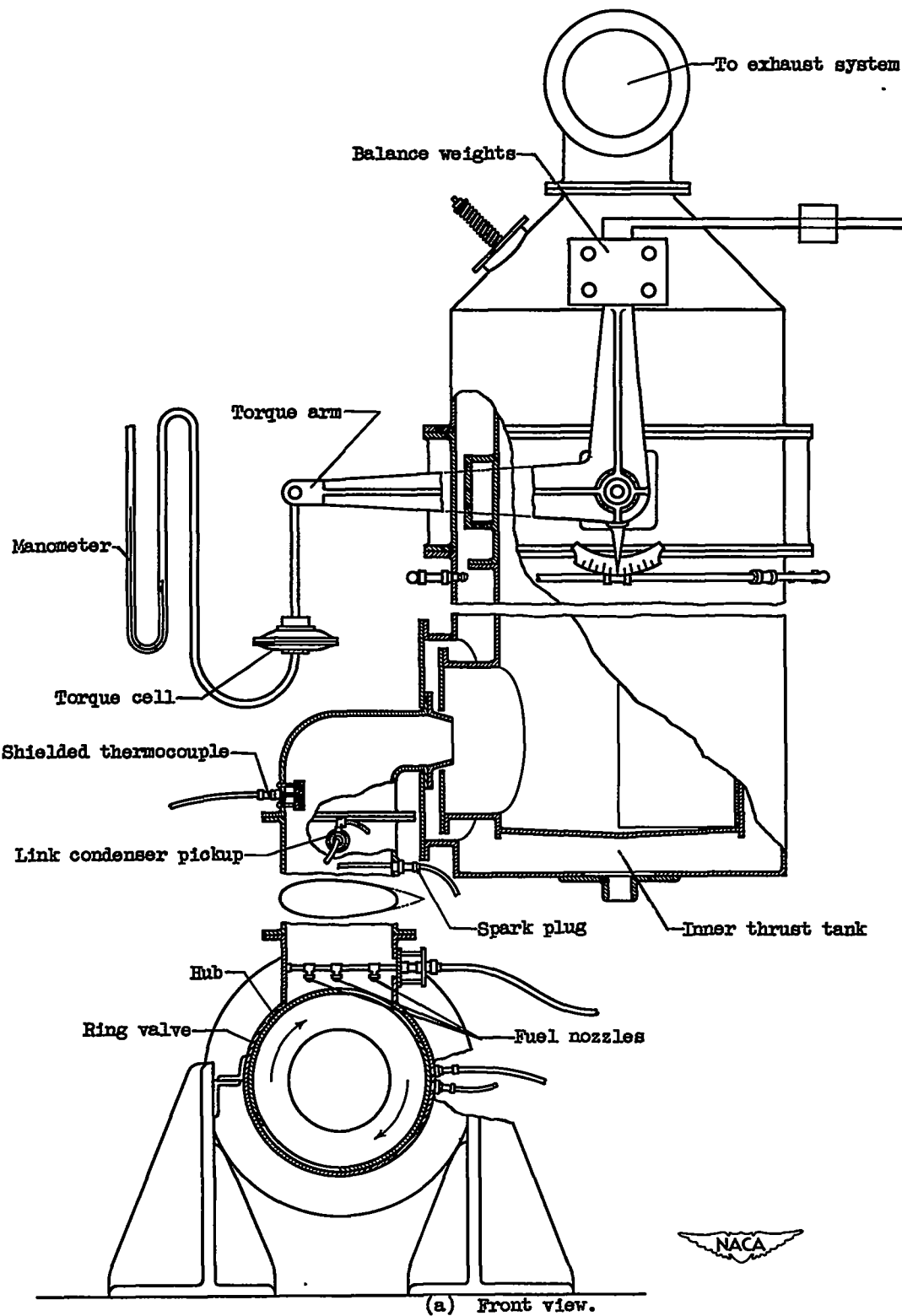


Figure 2. - Details of explosion-cycle combustion chamber and auxiliary equipment.

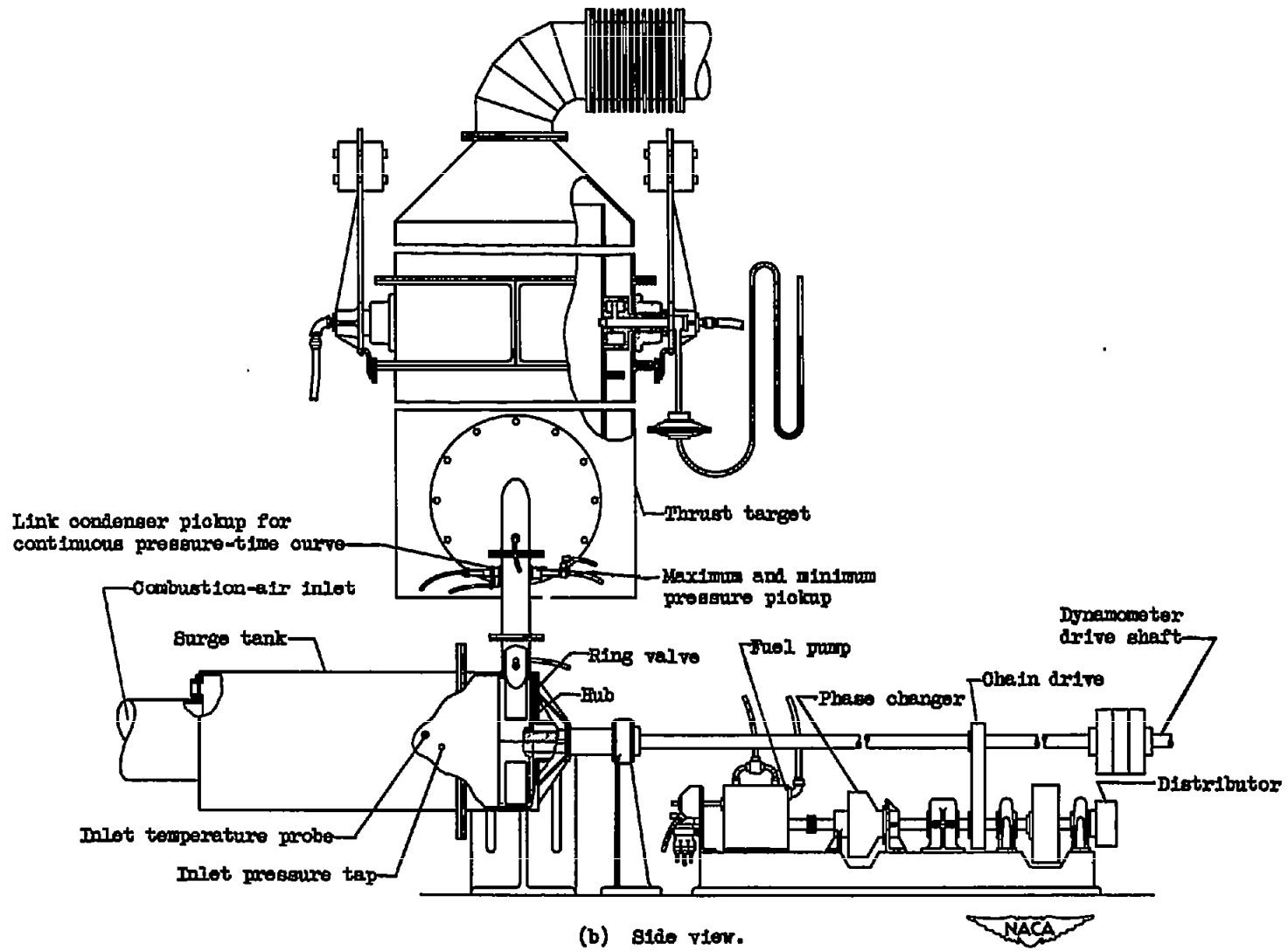
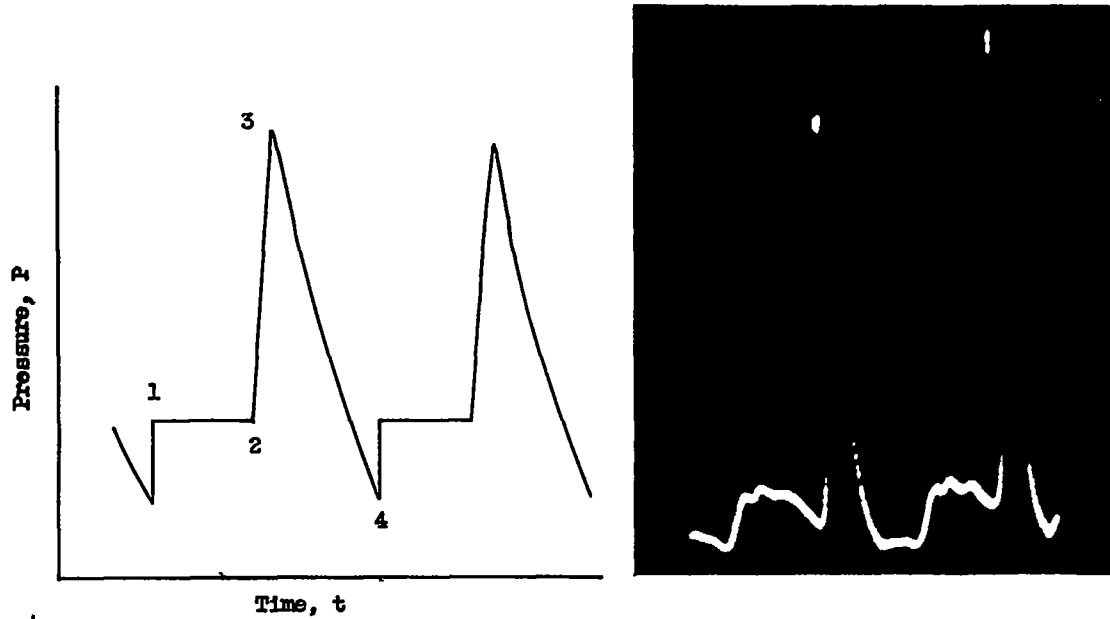
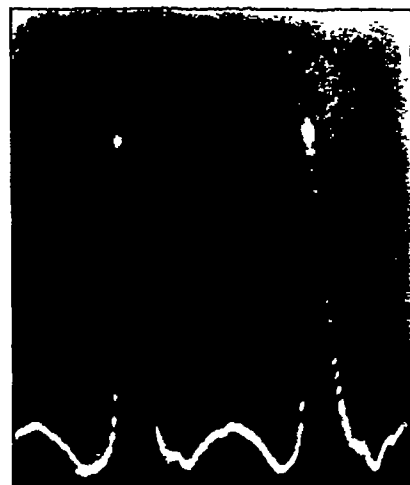
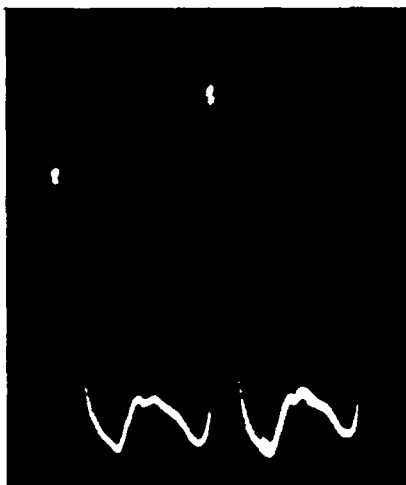


Figure 2. - Concluded. Details of explosion-cycle combustion chamber and auxiliary equipment.



(a) Ideal cycle.

$$(b) \frac{A_e}{A_b} = \frac{1}{9}.$$



$$(c) \frac{A_e}{A_b} = \frac{1}{6}.$$

$$(d) \frac{A_e}{A_b} = \frac{1}{4}.$$



C-21206
4-19-48

Figure 3. - Typical pressure-time diagrams for several ratios of exhaust-nozzle area to combustion-chamber cross-sectional area A_e/A_b . (For explanation of number stations in fig. 3(a) see appendix A.)



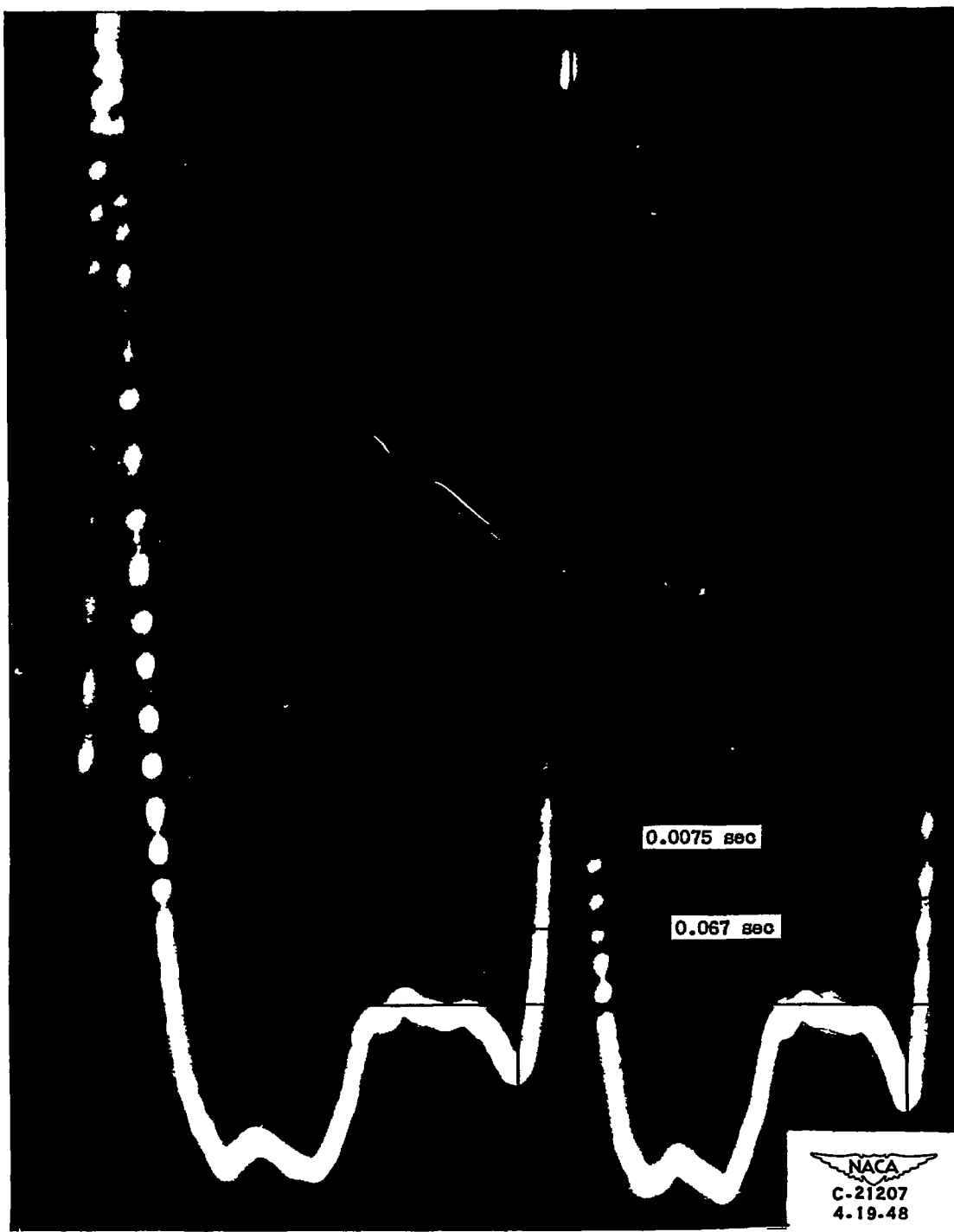
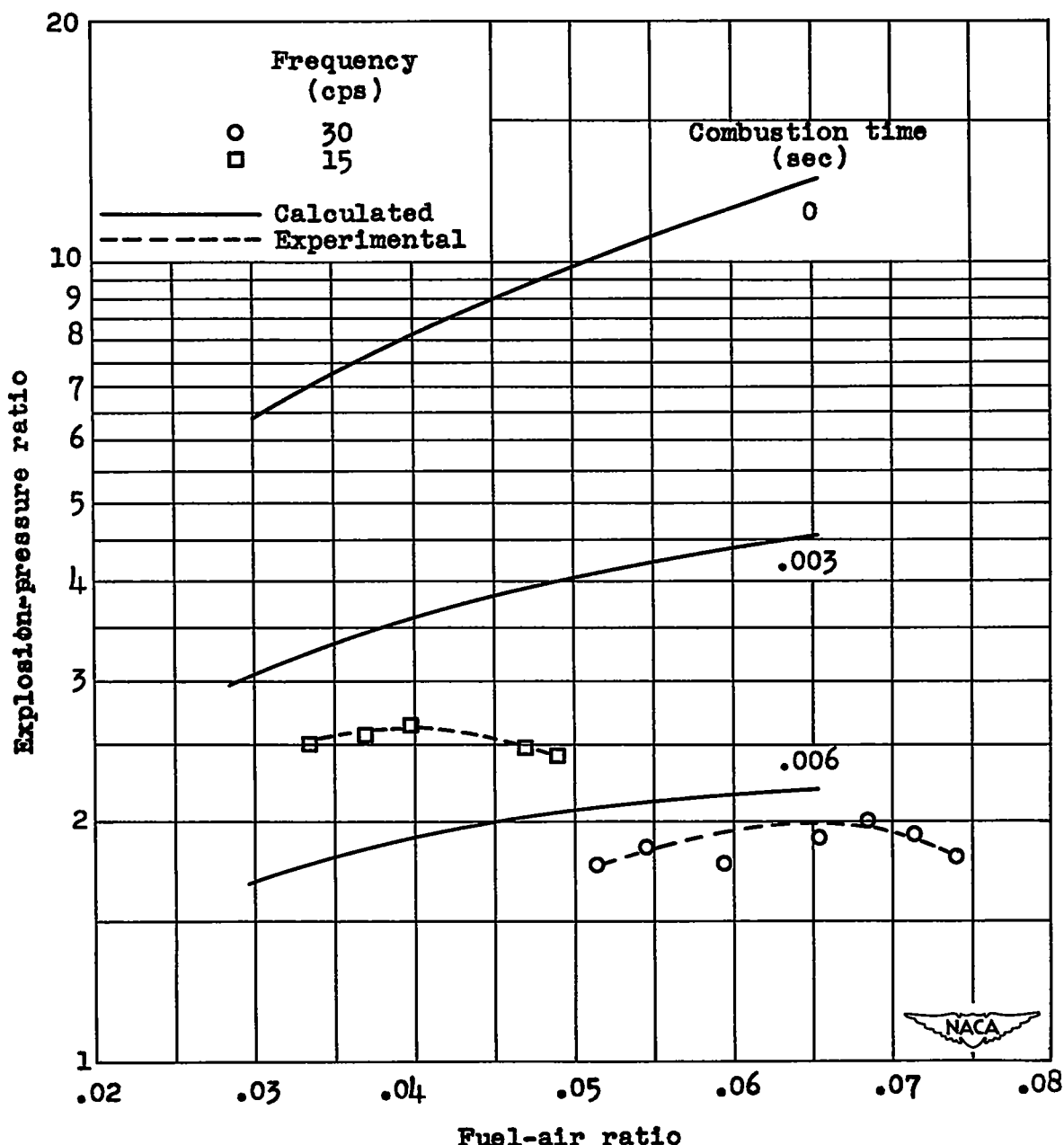


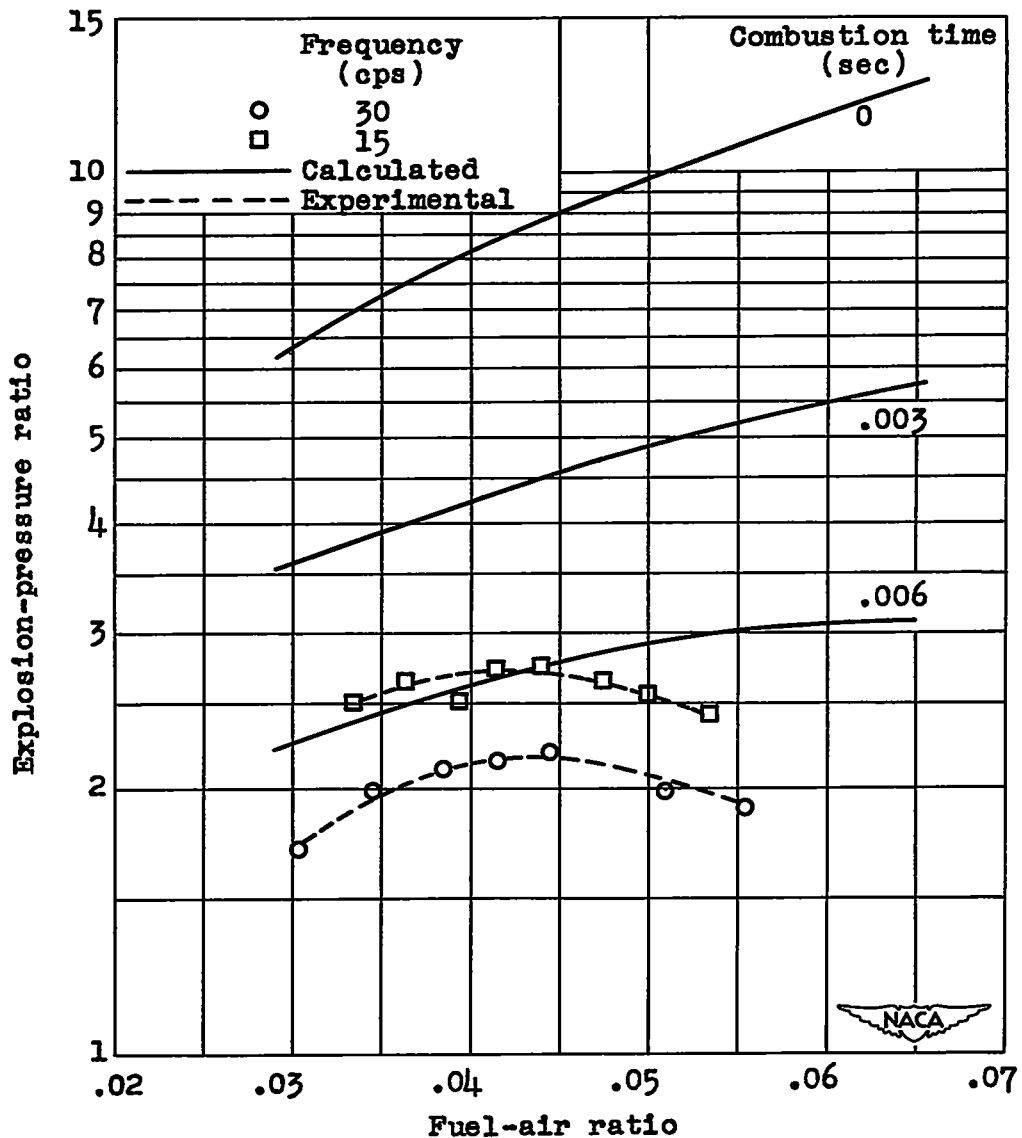
Figure 4. - Enlarged photograph of pressure-time diagram showing method of estimating combustion time. Frequency, 15 cycles per second.





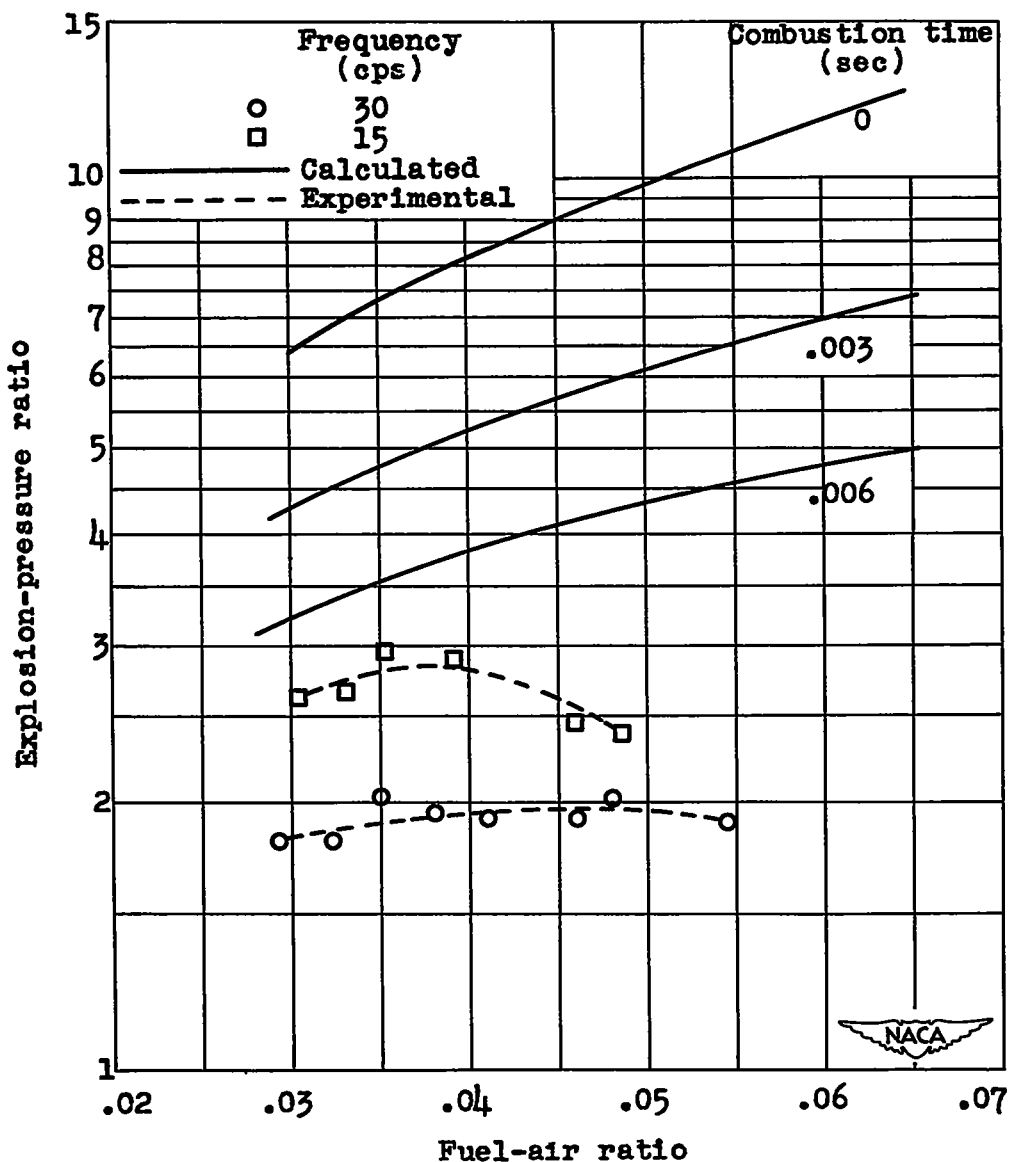
(a) Ratio of exhaust-nozzle area to combustion-chamber cross-sectional area A_e/A_b , 1/3.

Figure 5. - Comparison of experimentally determined values of explosion-pressure ratio with calculated values for range of fuel-air ratios and for several ratios of exhaust-nozzle area to combustion-chamber cross-sectional area. Inlet-pressure ratio, 1.2.



(b) Ratio of exhaust-nozzle area to combustion-chamber cross-sectional area A_e/A_b , 1/4.

Figure 5. - Continued. Comparison of experimentally determined values of explosion-pressure ratio with calculated values for range of fuel-air ratios and for several ratios of exhaust-nozzle area to combustion-chamber cross-sectional area. Inlet-pressure ratio, 1.2.



(c) Ratio of exhaust-nozzle area to combustion-chamber cross-sectional area A_e/A_b , 1/6.

Figure 5. - Concluded. Comparison of experimentally determined values of explosion-pressure ratio with calculated values for range of fuel-air ratios and for several ratios of exhaust-nozzle area to combustion-chamber cross-sectional area. Inlet-pressure ratio, 1.2.

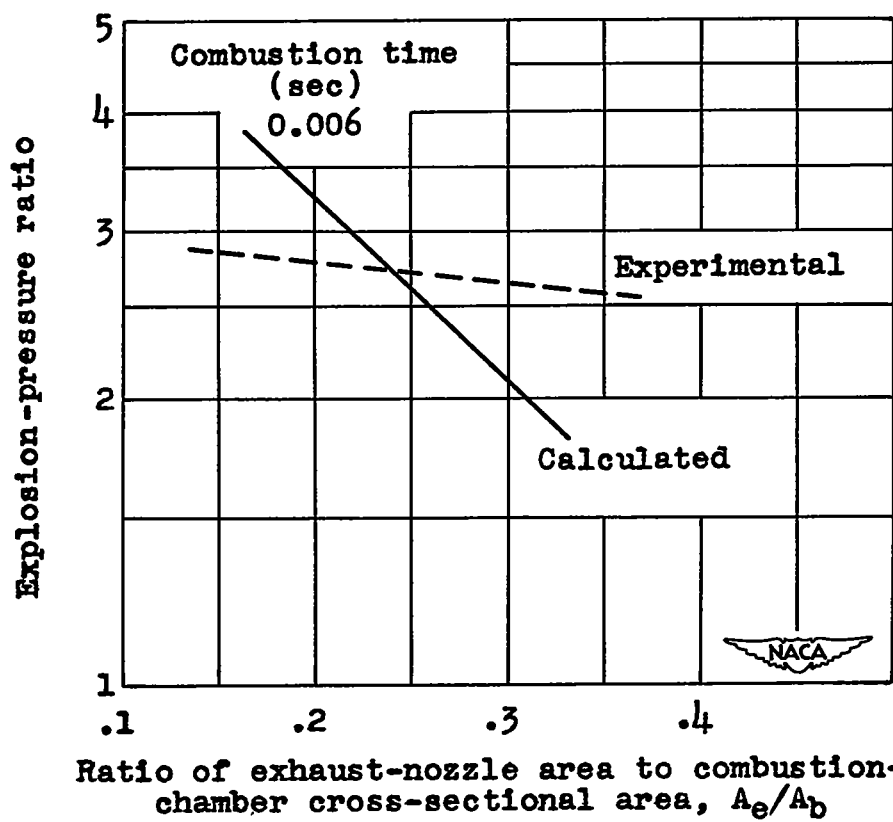


Figure 6. - Effect of ratio of exhaust-nozzle area to combustion-chamber cross-sectional area on explosion-pressure ratio. Inlet-pressure ratio, 1.2; fuel-air ratio, 0.04; cycle frequency, 15 cycles per second.

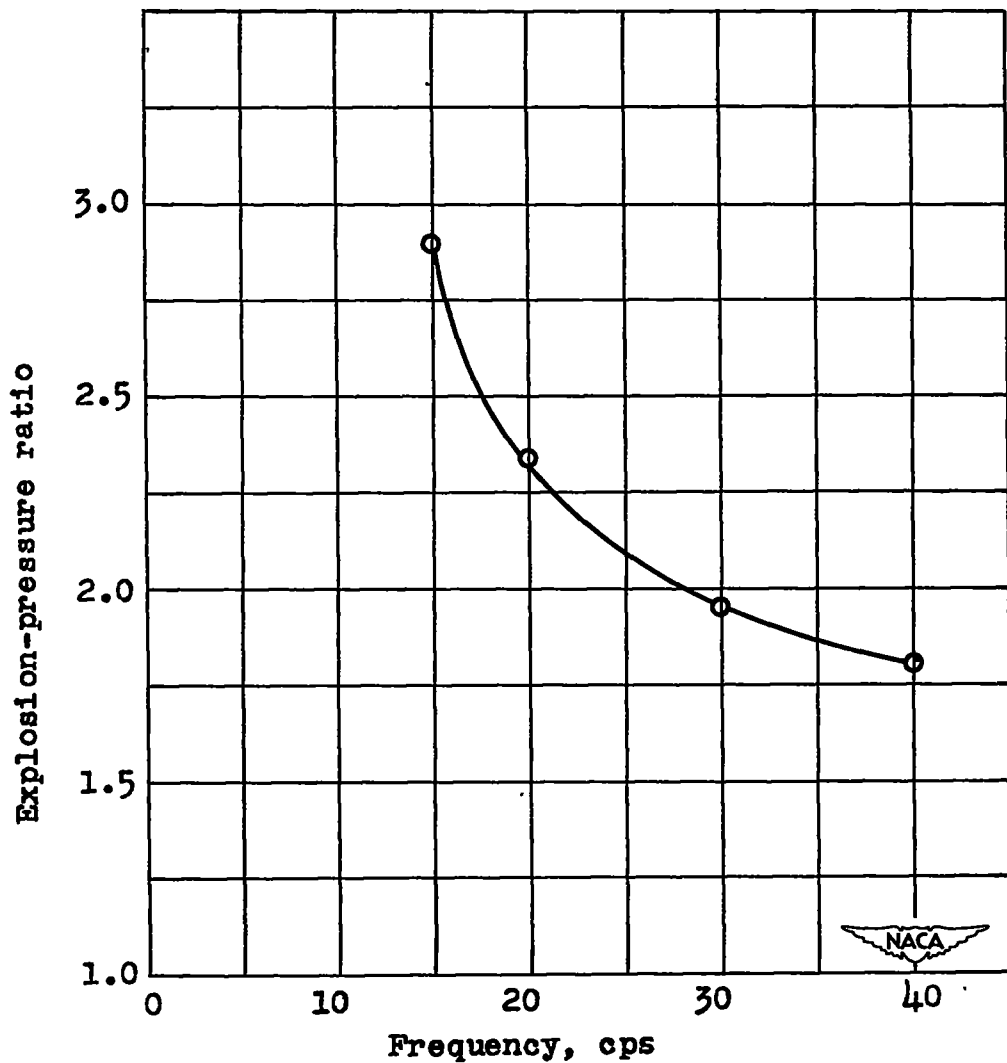


Figure 7. - Effect of cycle frequency on explosion-pressure ratio. Ratio of exhaust-nozzle area to combustion-chamber cross-sectional area, 1/6; fuel-air ratio, 0.04; inlet-pressure ratio, 1.2.

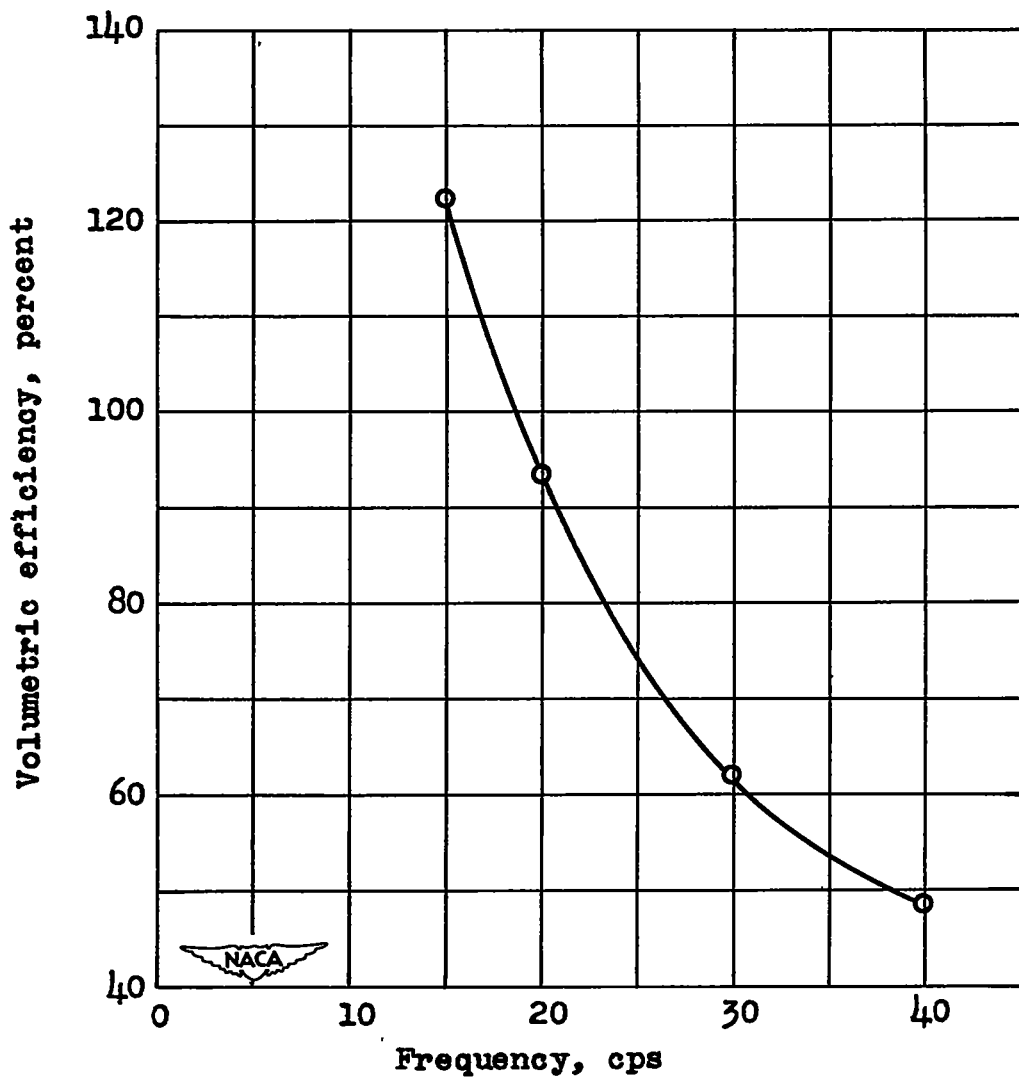


Figure 8. - Effect of cycle frequency on volumetric efficiency. Ratio of exhaust-nozzle area to combustion-chamber cross-sectional area, 1/6; fuel-air ratio, 0.04; inlet-pressure ratio, 1.2.

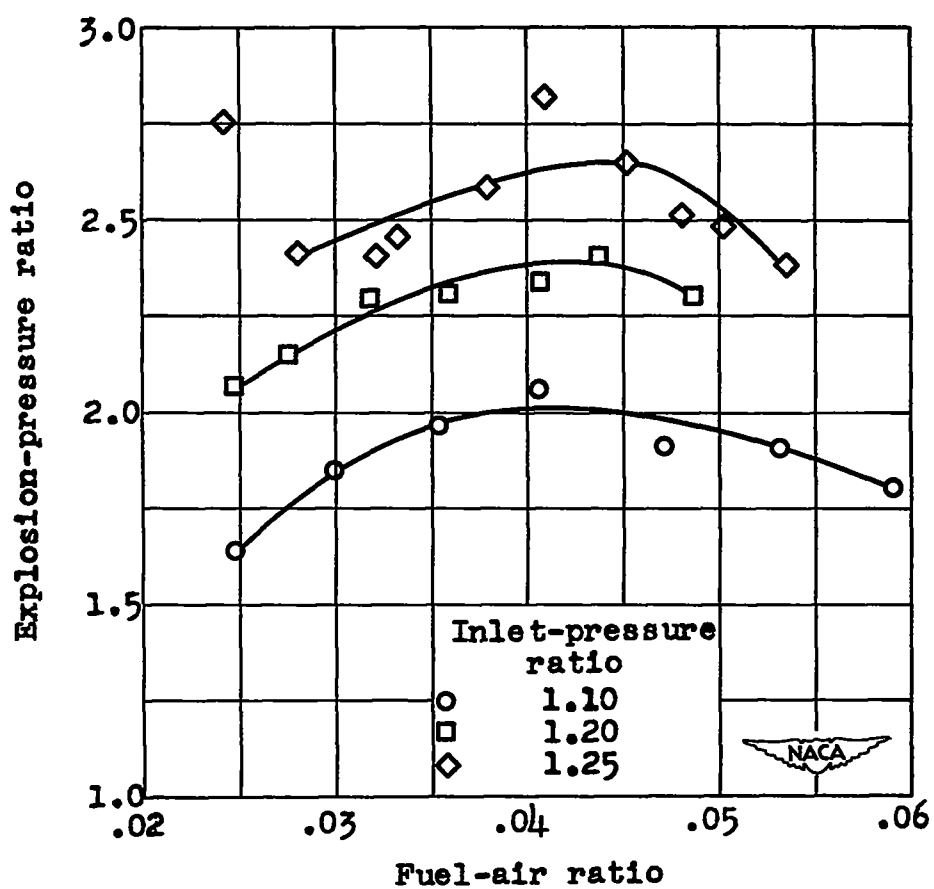
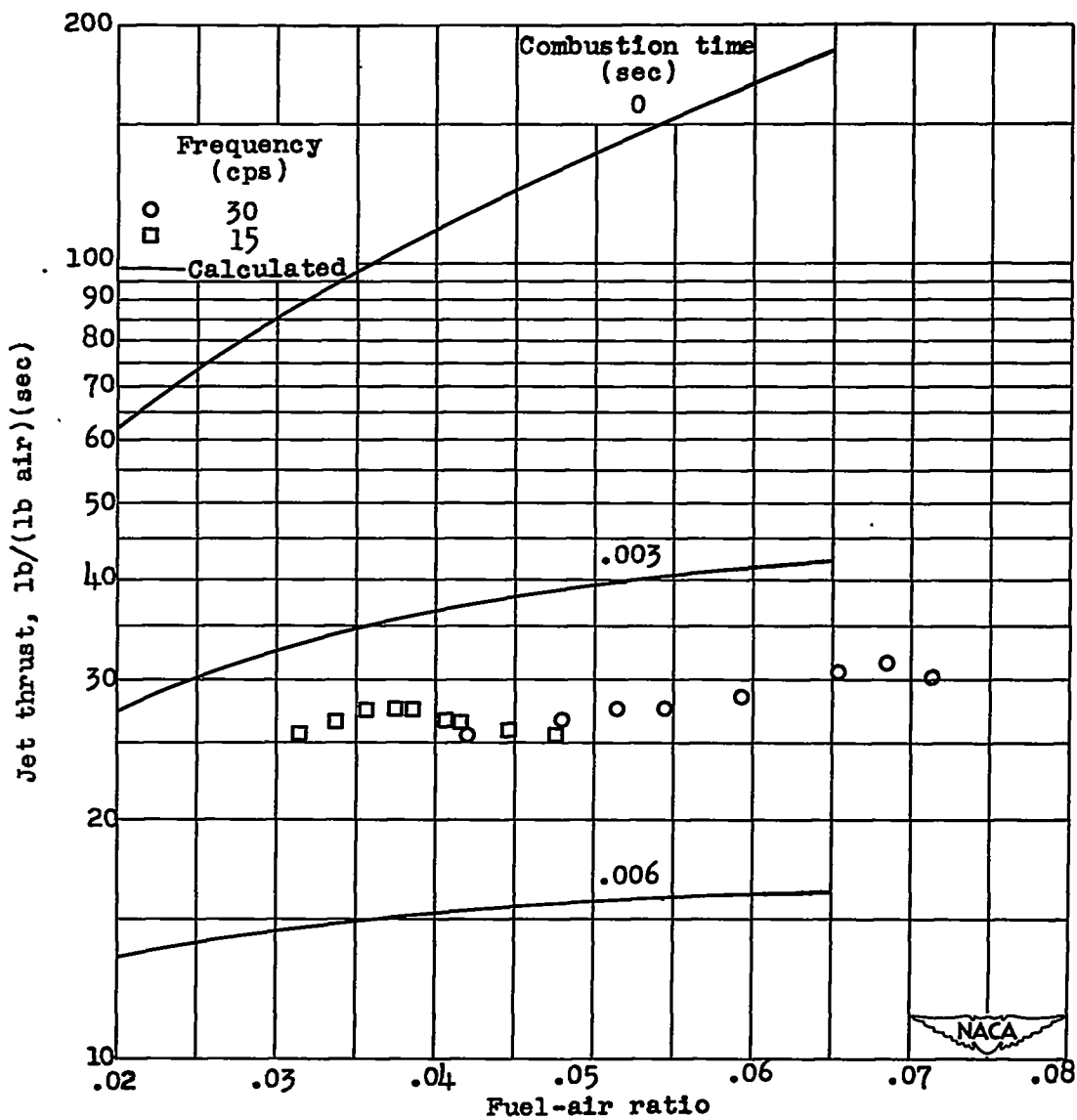
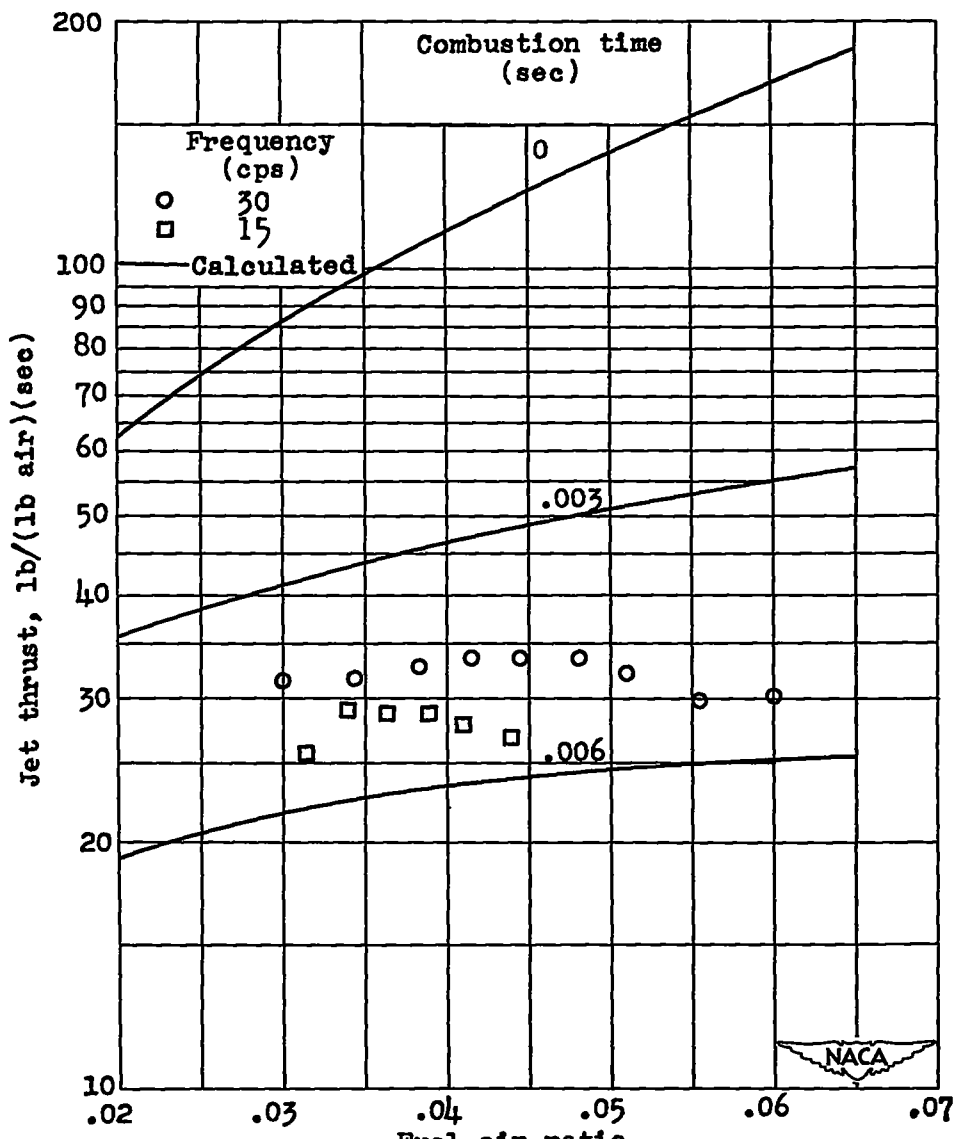


Figure 9. - Effect of inlet-pressure ratio on explosion-pressure ratio. Ratio of exhaust-nozzle area to combustion-chamber cross-sectional area, 1/6; cycle frequency, 20 cycles per second.



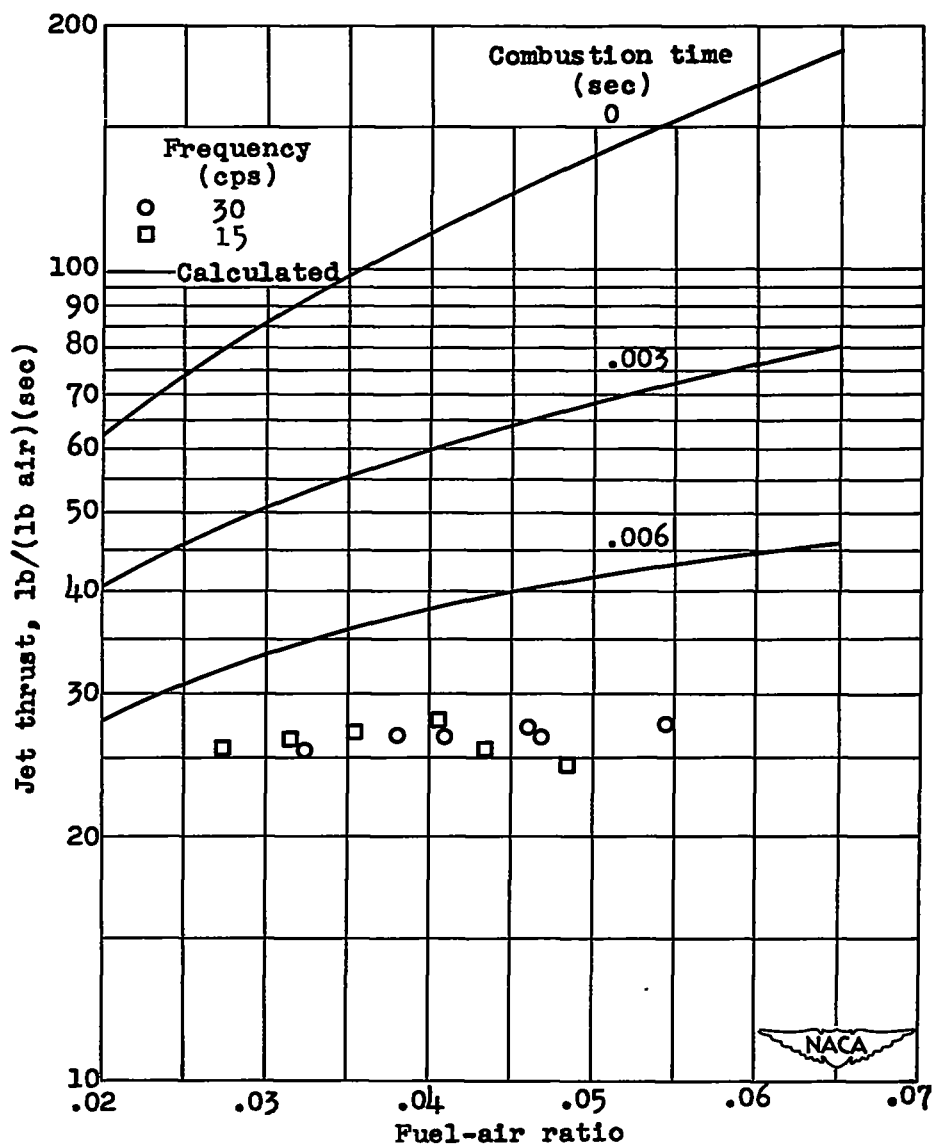
(a) Ratio of exhaust-nozzle area to combustion-chamber cross-sectional area A_e/A_b , 1/3.

Figure 10. - Variation of experimental and calculated jet thrust per pound of air with fuel-air ratio for several ratios of exhaust-nozzle area to combustion-chamber cross-sectional area. Inlet-pressure ratio, 1.2.



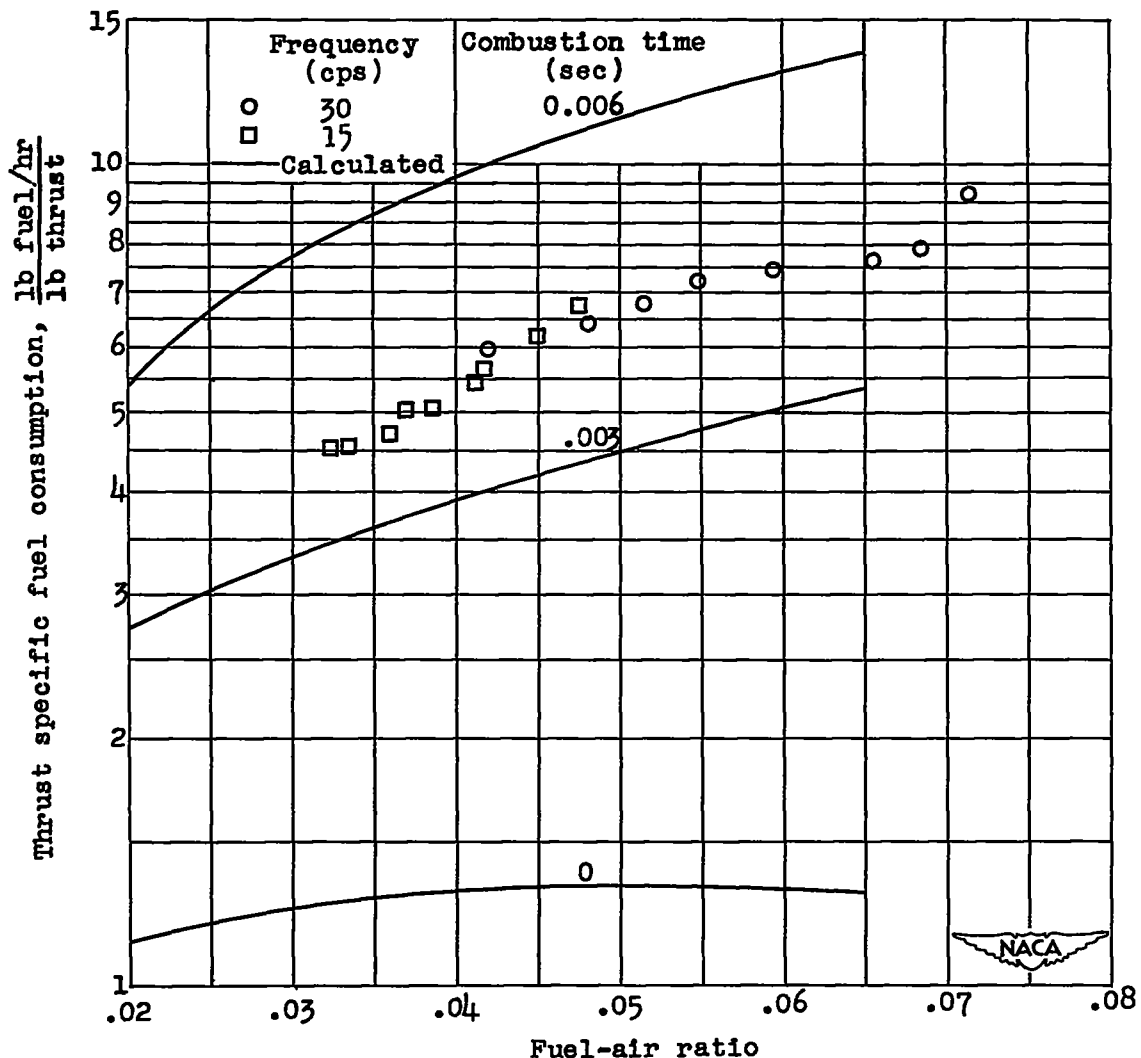
(b) Ratio of exhaust-nozzle area to combustion-chamber cross-sectional area A_e/A_b , 1/4.

Figure 10. - Continued. Variation of experimental and calculated jet thrust per pound of air with fuel-air ratio for several ratios of exhaust-nozzle area to combustion-chamber cross-sectional area. Inlet-pressure ratio, 1.2.



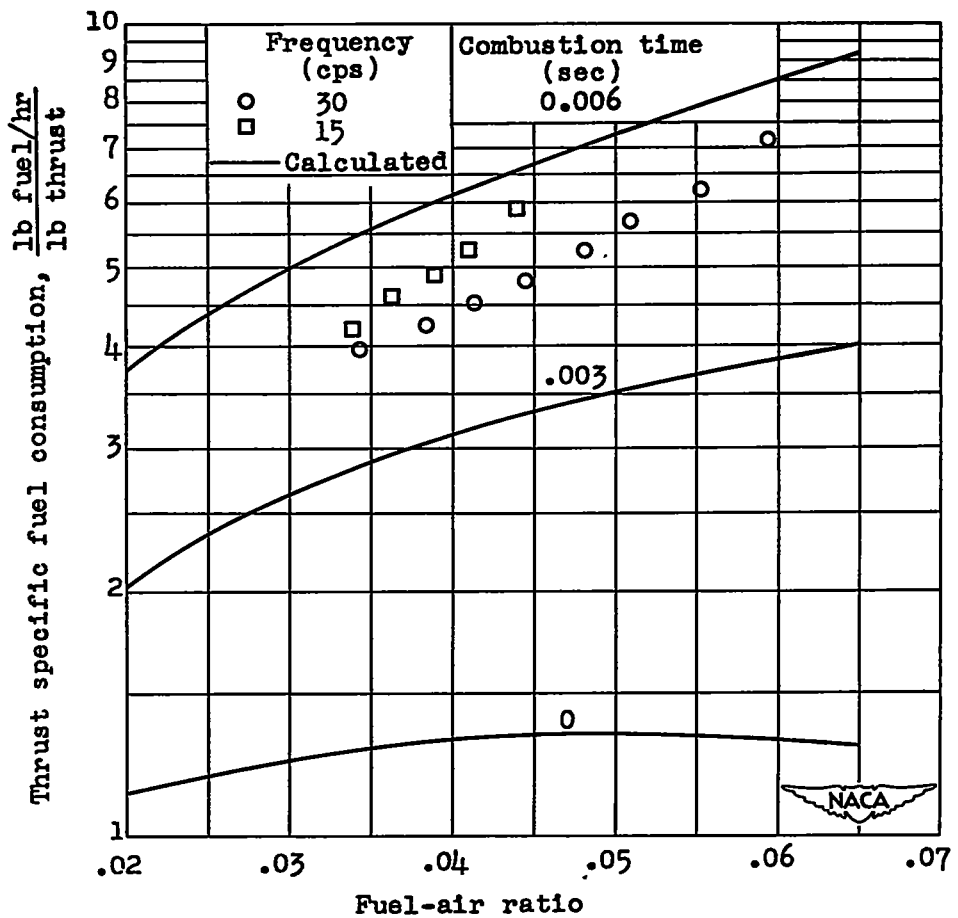
(c) Ratio of exhaust-nozzle area to combustion-chamber cross-sectional area A_e/A_b , 1/6.

Figure 10. - Concluded. Variation of experimental and calculated jet thrust per pound of air with fuel-air ratio for several ratios of exhaust-nozzle area to combustion-chamber cross-sectional area. Inlet-pressure ratio, 1.2.



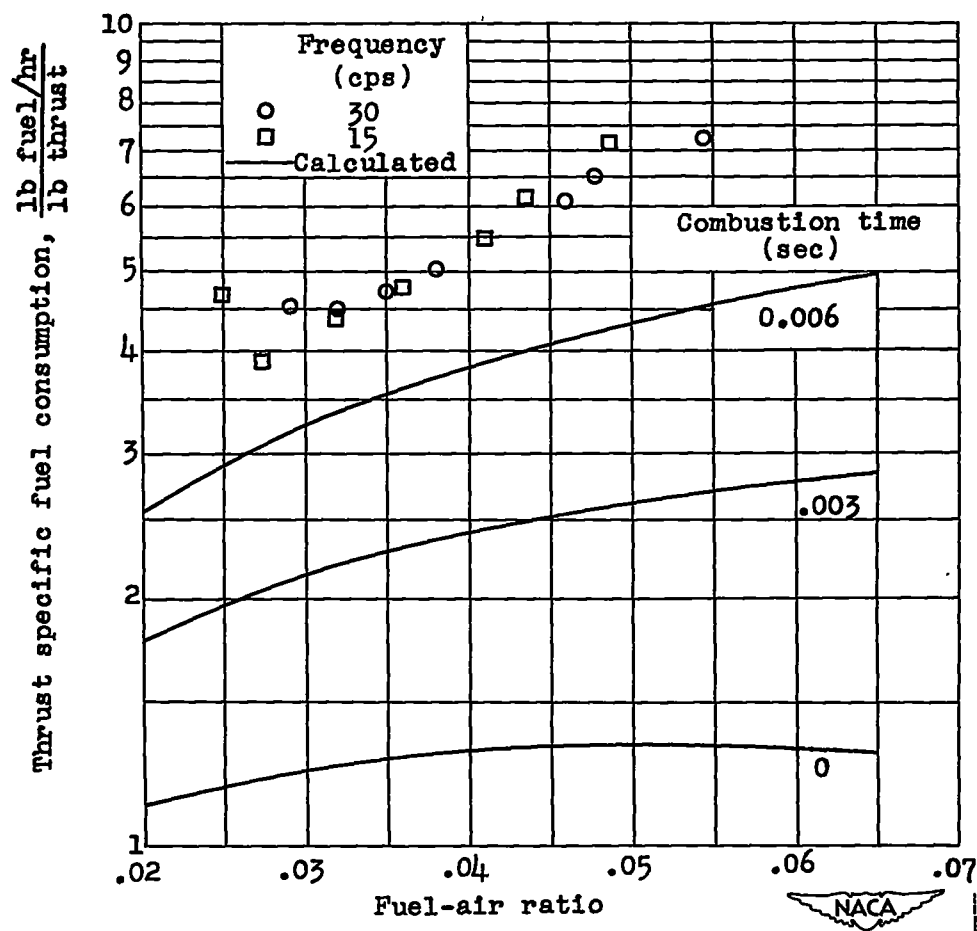
(a) Ratio of exhaust-nozzle area to combustion-chamber cross-sectional area A_e/A_b , 1/3.

Figure 11. Variation of experimental and calculated thrust specific fuel consumption with fuel-air ratio for several ratios of exhaust-nozzle area to combustion-chamber cross-sectional area. Inlet-pressure ratio, 1.2.



(b) Ratio of exhaust-nozzle area to combustion-chamber cross-sectional area A_e/A_b , 1/4.

Figure 11. - Continued. Variation of experimental and calculated thrust specific fuel consumption with fuel-air ratio for several ratios of exhaust-nozzle area to combustion-chamber cross-sectional area. Inlet-pressure ratio, 1.2.



(c) Ratio of exhaust-nozzle area to combustion-chamber cross-sectional area A_e/A_b , 1/6.

Figure 11. - Concluded. Variation of experimental and calculated thrust specific fuel consumption with fuel-air ratio for several ratios of exhaust-nozzle area to combustion-chamber cross-sectional area. Inlet-pressure ratio, 1.2.